Electronic Supplementary Material (ESI) for Chemical Communications.

Electronic Supporting Information

Tolerant to Air σ-Alkane Complexes by Surface Modification of Single Crystalline Solid-State Molecular Organometallics Using Vapour-Phase Cationic Polymerisation: SMOM@Polymer

Alexander J. Bukvic,[a,b] Dana-Georgiana Crivoi,[a] Hollie G. Garwood,[a] Alasdair I. Mckay,[a] Thomas T. D. Chen,[a] Antonio J. Martinez-Martinez[a] and Andrew S. Weller. [a,b]

a: *Department of Chemistry, Chemistry Research Laboratories, University of Oxford, OX1 3TA, U.K.*

b: *Department of Chemistry, University of York, YO10 5DD, U.K.*

E-mail: andrew.weller@york.ac.uk

Table of Contents

S.1. Experimental Details

S.1.1. General Methods

All manipulations (unless otherwise stated) were performed under an atmosphere of argon, using standard Schlenk techniques on a dual vacuum/inlet manifold or by use of an MBraun glovebox. Glassware was dried in an oven at 130 °C overnight prior to use. Pentane, diethyl ether ($C_4H_{10}O$) and dichloromethane (CH_2Cl_2) were dried using an MBraun SPS-800 solvent purification system and degassed by three freeze-pump-thaw cycles. 1,2-$F_2C_6H_4$ (abbreviated as $F_2C_6H_4$) was stirred over Al_2O_3 for two hours then over CaH_2 overnight before being vacuum distilled and subsequently degassed by three freeze- pump-thaw cycles. D_2-dichloromethane (abbreviated as CD_2Cl_2) and d_3-acetonitrile (abbreviated to d_3-MeCN) were dried by stirring over CaH_2 overnight before being vacuum distilled onto 3 Å molecular sieves and subsequently degassed by three freeze-pump-thaw cycles. Ethyl Vinyl Ether (EVE) was purchased from Sigma-Aldrich and was stirred over Na pieces overnight before being vacuum distilled and subsequently degassed by three freeze-pump-thaw cycles before use. All other chemicals were purchased from commercial vendors and used as received.

$[Rh(Cy_2PCH_2CH_2PCy_2)(F_2C_6H_4)][BAr^F_4]$[S1] **$[1\text{-}F_2C_6H_4][BAr^F_4]$**, $[Rh(Cy_2PCH_2CH_2PCy_2)(NBD)][BAr^F_4]$[S2] (NBD = norbornadiene) **$[1\text{-NBD}][BAr^F_4]$**, and $Rh(Cy_2PCH_2CH_2PCy_2)(NBA)][BAr^F_4]$[S2] (NBA = norborane) **$[1\text{-NBA}][BAr^F_4]$** were prepared by the literature procedures.

Solution NMR data were collected on either a Bruker AVD 500 MHz or a Bruker Ascend 400 MHz spectrometer at room temperature unless otherwise started. Non-deuterated solvents were locked to standard external CD_2Cl_2 solutions. Residual protio solvent resonances were used as a reference for ^{1}H NMR spectra. $^{31}P\{^1H\}$ NMR spectra were referenced externally to 85 % H_3PO_4 (D_2O). All chemical shifts (δ) are quoted in ppm and coupling constants in Hz.

Solid state NMR (SSNMR) samples were prepared by packing powdered microcrystalline sample into a 4 mm zirconia solid state rotor inside an argon filled glove box. SSNMR spectra were obtained on a Bruker Avance III HD spectrometer equipped with a 9.4 Tesla magnet, operating at 100.6 MHz for ^{13}C and 62 MHz for ^{31}P, respectively, and a MAS rate of 10 kHz. Relaxation time for ^{1}H and contact time for $^{31}P\{^1H\}$ CP/MAS and $^{13}C\{^1H\}$ CP/MAS NMR experiments were optimized for each compound as appropriate. All $^{13}C\{^1H\}$ CP/MAS spectra were referenced to adamantane (upfield methine resonance, δ = 29.5 ppm)[S3] on a scale where δ (TMS) = 0 ppm as a secondary reference.

Scanning electron microscopy (SEM) was performed using a Carl Zeiss Merlin– Analytical instrument, with an operating voltage of 5 kV. The samples were prepared by selecting crystals and mounting directly on carbon tape within an argon filled glove box. The samples were rapidly transferred to the main chamber of the instrument under air, then immediately placed under vacuum.

Energy dispersive X-ray spectroscopy (EDX), carried out on a Carl Zeiss Merlin– Analytical instrument with an operating voltage of 5 kV or 3 kV, was used to identify the elements found in the materials.

SEC (GPC) data was obtained using a Shimadzu LC-20AD instrument fitted with a refractive index (RI) detector. HPLC grade THF was used as the eluent, flowing at 1.0 mL/min at 30 °C and samples calibrated to monodisperse polystyrene standard.

S.2. Synthetic Procedures

S.2.1. $[Rh(Cy_2P(CH_2)_2PCy_2)(NBA)][BAr^F{}_4]$@polymer; $[1\text{-}NBA][BAr^F{}_4]$@poly(ethylvinylether)

Method B

To Mount: Inside an argon filled glove box, crystals of **[1-NBD]**$[\mathbf{BAr^F{}_4}]$ (Typically 5 x crystals of approximately 1 mg each, with an approximate size of 1 x 1 x 1.5 mm) were mounted to a specially adapted J. Young tap, shown in Figure S1. This was constructed from a cut needle gently pressed into the base of the J. Young tap, and was lightly covered in silicon grease to aid attachment of the **[1-NBD]**$[\mathbf{BAr^F{}_4}]$ crystals.

Once mounted: A J. Young flask (~ 50 mL) was sealed with the adapted J. Young tap with mounted crystals and evacuated ($< 3 \times 10^{-2}$ mbar), filled with H_2 gas (15 psi, 298 K) and left to stand for 60 mins, to form **[1-NBA]**$[\mathbf{BAr^F{}_4}]$ *in-situ*.[S2] Care was taken to not dislodge any crystals from the mount during gas evacuation and addition.

After this time, the H_2 was removed under vacuum ($< 3 \times 10^{-2}$ mbar) and flask cooled to 77 K using liquid nitrogen. Ethyl Vinyl Ether (EVE) (0.1 mL) was then vacuum distilled into the flask, and rapidly warmed to room temperature, at which the volatility of EVE (b.p. 33 ºC) allowed for an atmosphere of EVE to be formed as a timer was started. After set time periods of either 30 seconds, 2.5 minutes, or 15 minutes at ambient temperature, the flask was again placed under vacuum ($< 3 \times 10^{-2}$ mbar) to remove excess ethyl vinyl ether and back filled with argon to yield $[Rh(Cy_2P(CH_2)_2PCy_2)(NBA)][BAr^F{}_4]$@polymer; **[1-NBA]**$[\mathbf{BAr^F{}_4}]$**@poly(ethylvinylether)**.

[1-NBA]$[\mathbf{BAr^F{}_4}]$**@poly(ethylvinylether)** was analysed by ^1H and $^{31}P\{^1H\}$ solution NMR spectroscopy, $^{31}P\{^1H\}$ and $^{13}C\{^1H\}$ Solid-State NMR spectroscopy, single crystal x-ray diffraction and SEM / EDX experiments.

Note: Due to the fragile nature of the crystals, it was found **[1-NBA]**$[\mathbf{BAr^F{}_4}]$ could not be easily handled or mounted, hence stronger crystals of **[1-NBD]**$[\mathbf{BAr^F{}_4}]$ were mounted and hydrogenated *in situ* to give **1-NBA]**$[\mathbf{BAr^F{}_4}]$.

It was also found **[1-NBD]**$[\mathbf{BAr^F{}_4}]$ does not initiate the polymerisation of ethyl vinyl ether. **[1-NBA]**$[\mathbf{BAr^F{}_4}]$ was essential for initiation.

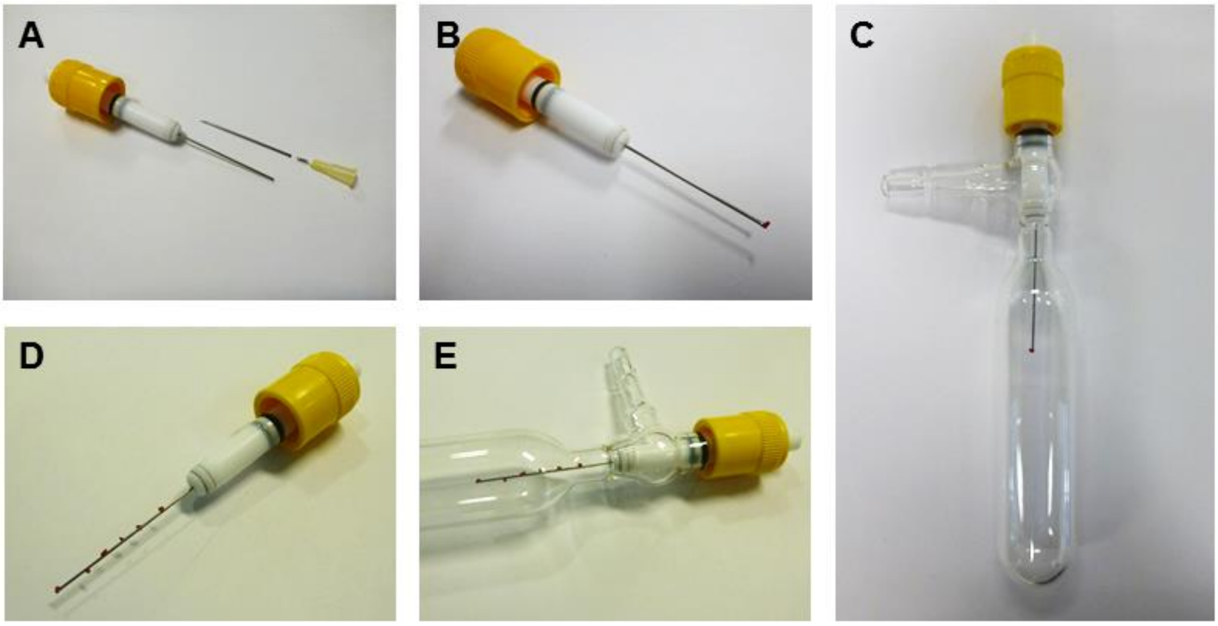

Figure S1: **(A)** Set up of specially adapted J. Young tap, involving cut needle pressed into the base of tap. **(B)** Adapted tap with 1 x 1 mg crystal of **[1-NBD][BAr$^F_4$]** attached to end of needle. **(C)** Full construction inserted into J. Young flask. **(D)** Adapted tap with multiple crystals mounted. **(E)** Full construction of mounted crystals into reaction flask.

S.2.2. [1-NBA][BAr$^F_4$]@poly(ethylvinylether) – Solution NMR Characterization

[1-NBA][BAr$^F_4$]@poly(ethylvinylether) (10 mgs) of material obtained after 30 seconds exposure time to an EVE atmosphere were dissolved in d_3-MeCN and analysed by ^1H and $^{31}P\{^1H\}$ NMR spectroscopy.

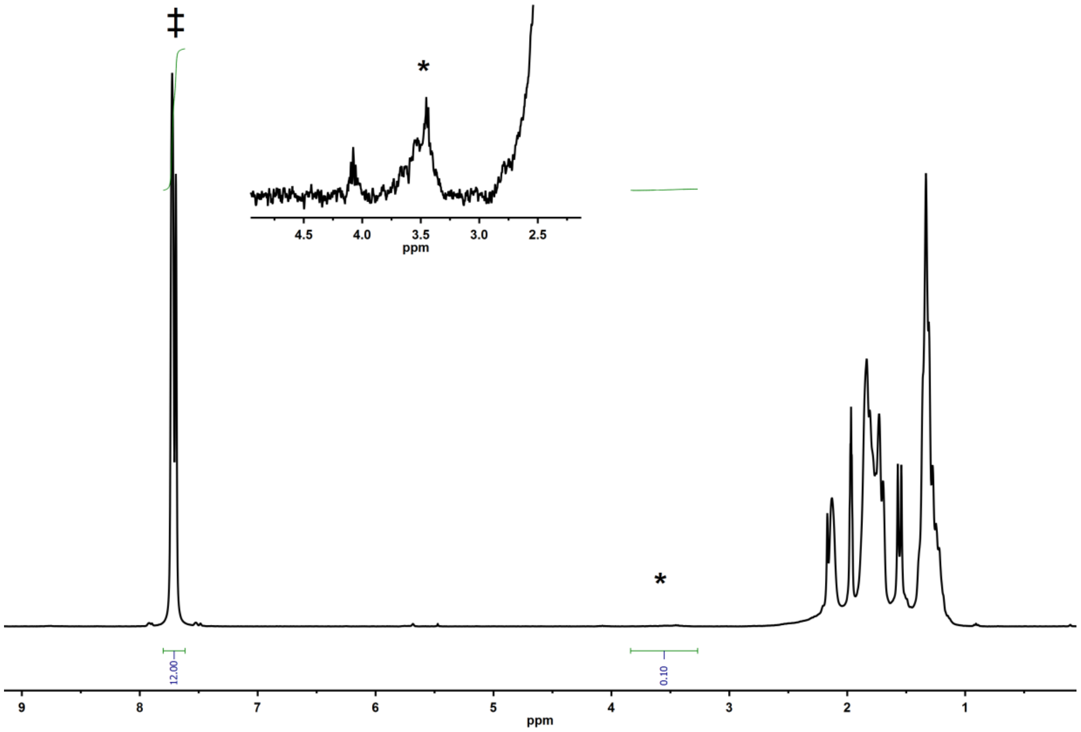

Figure S2: ^1H NMR spectrum (d_3-MeCN, 400 MHz, 298 K) of dissolved **[1-NBA][BAr$^F_4$]@poly(ethylvinylether)** after 30 seconds EVE exposure. Peaks marked * are from –OC**H**- and -OC**H$_2$**CH$_3$ resonances in the liberated polymer coating,[S4] confirming **poly(ethylvinylether)** is present. The signals marked ‡ are from the [BAr$^F_4$]$^-$ anion and the signals between δ 1.2 and 2.3 are from the remaining polymer environments, cyclohexyl-group resonances as well as free and coordinated MeCN.

Integration of polymer –OC**H**- and -OC**H$_2$**CH$_3$ signals to **[BAr$^F_4$]$^-$** anion signals give a ratio of **0.1: 1**.

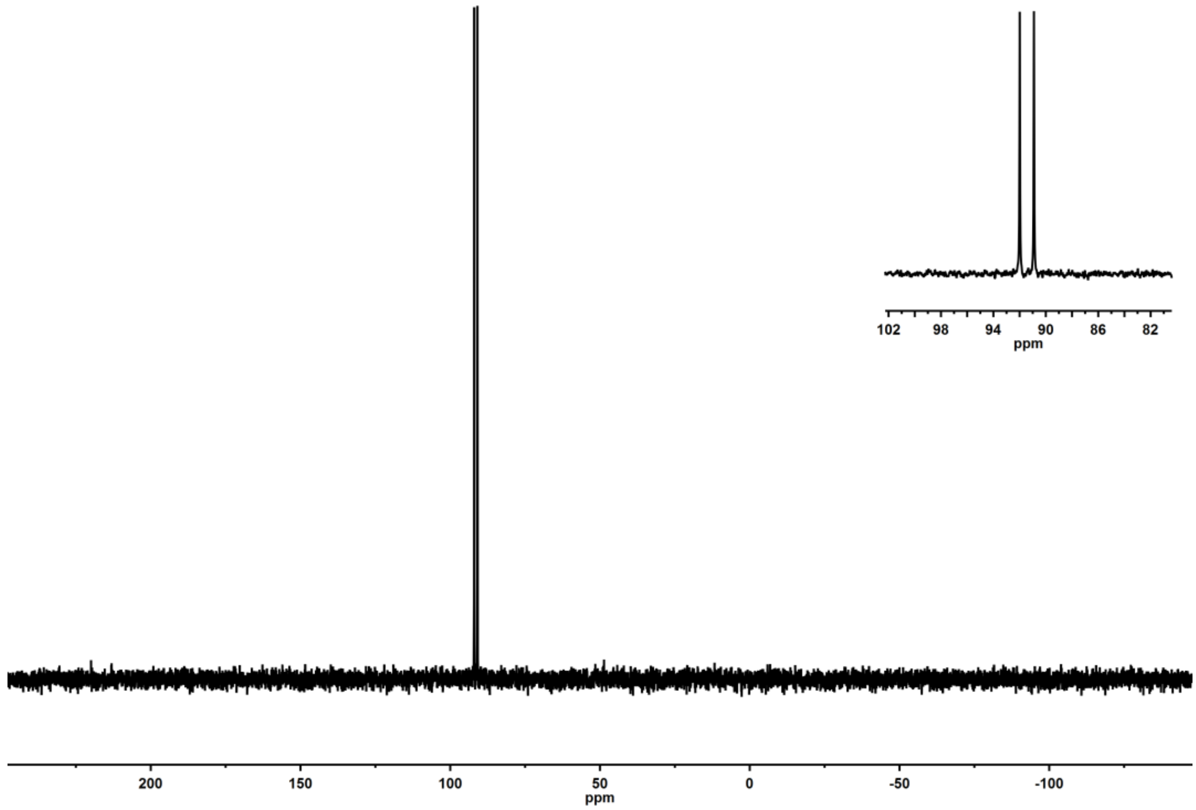

Figure S3: The $^{31}P\{^{1}H\}$ spectrum (d_3-MeCN, 162 MHz, 298 K) of dissolved **[1-NBA][BAr$^F{}_4$]@poly(ethylvinylether)** after 30 seconds EVE exposure to form [1-(MeCN)$_2$][BAr$^F{}_4$] shown by the doublet at δ 91 ($J_{Rh\text{-}P}$ = 175 Hz).[S5]

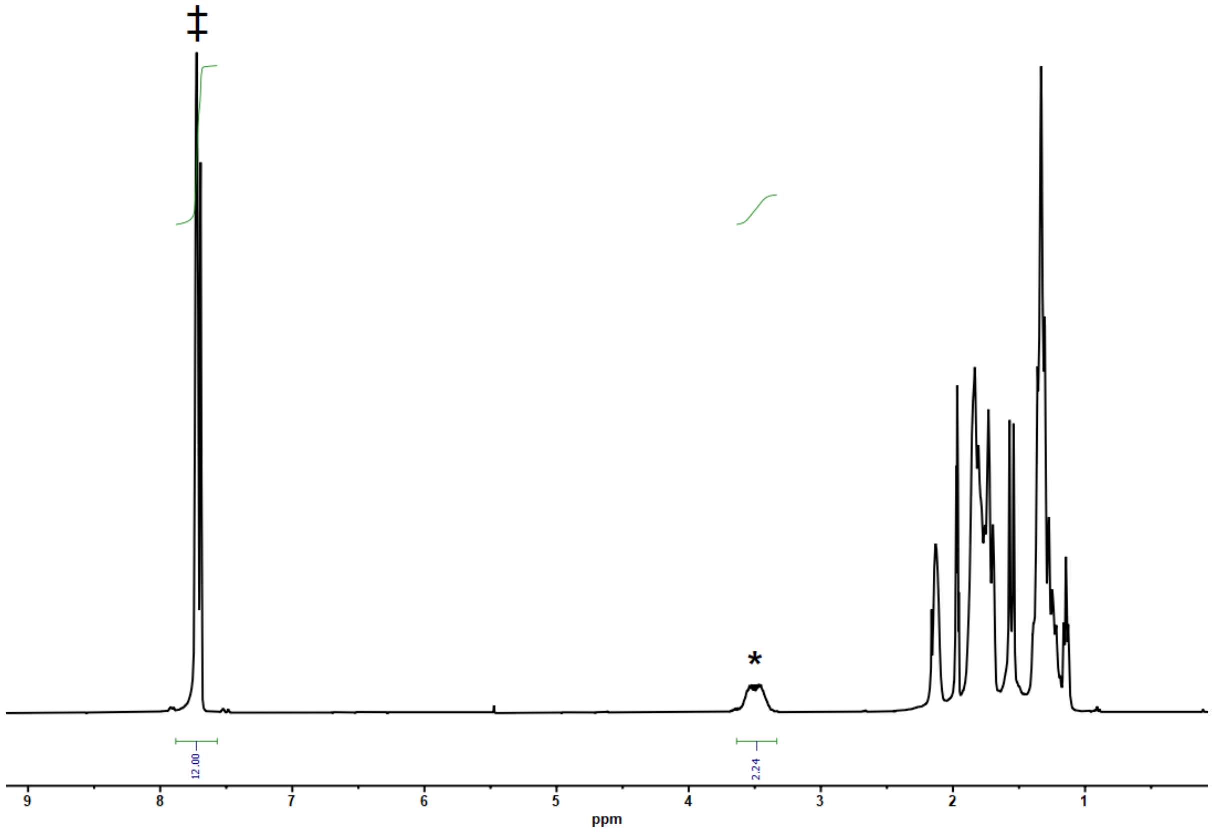

Figure S4: ^{1}H NMR spectrum (d_3-MeCN, 400 MHz, 298 K) of dissolved **[1-NBA][BAr$^{F}{}_{4}$]@poly(ethylvinylether)** after 2.5 minutes exposure. Peaks marked * are from the polymer produced, confirming **poly(ethylvinylether)** is present, and peaks marked ‡ are from the [BAr$^{F}{}_{4}$]$^{-}$ anion. No signals from EVE monomer can be observed.

Integration of polymer –OC**H**- and -OC**H$_2$**CH$_3$ signals to **[BAr$^{F}{}_{4}$]$^{-}$** anion signals give a ratio of **0.7: 1**.

Note: The $^{31}P\{^{1}H\}$ spectrum for 2.5 minutes coating was identical to that in Figure S3.

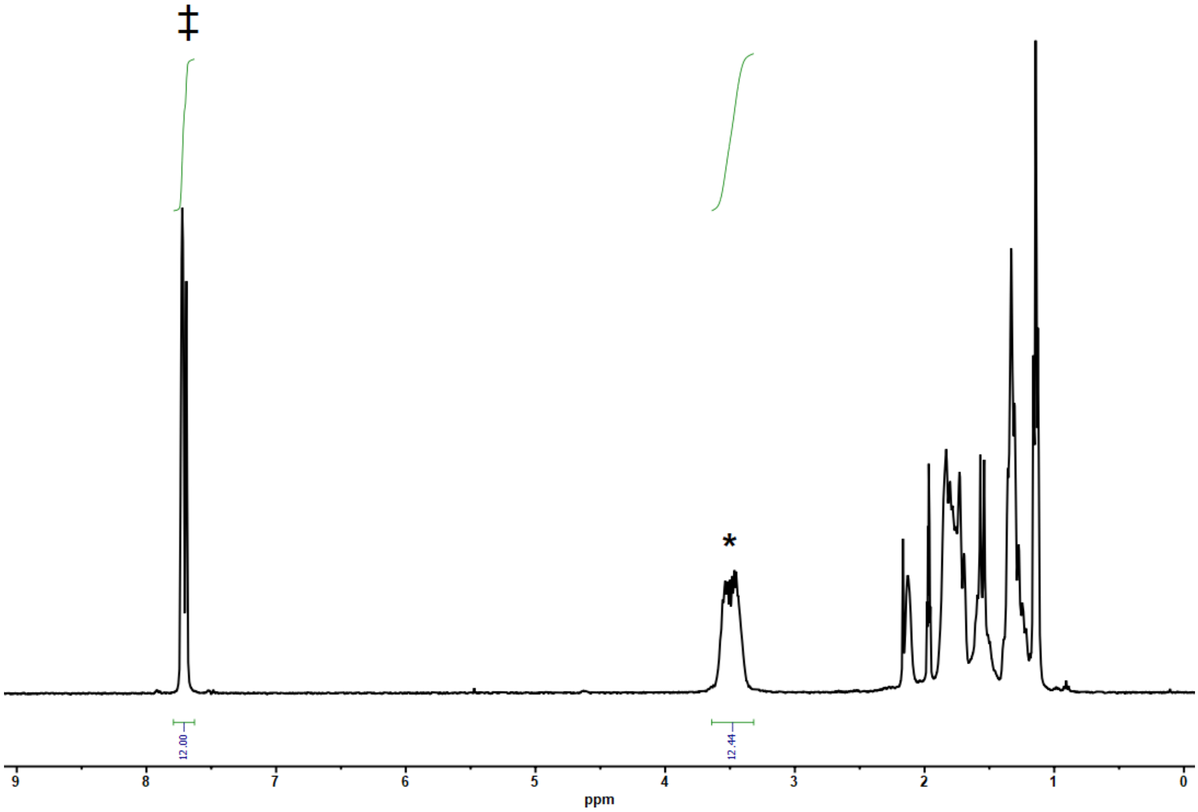

Figure S5: ^{1}H NMR spectrum (d_3-MeCN, 400 MHz, 298 K) of dissolved **[1-NBA][BAr$^F{}_4$]@poly(ethylvinylether)** after 15 minutes exposure. Peaks marked * are from the polymer produced, confirming **poly(ethylvinylether)** is present, and peaks marked ‡ are from the [BAr$^F{}_4$]$^-$ anion. No signals from EVE monomer can be observed.

Integration of polymer –OC**H**- and -OC**H$_2$**CH$_3$ signals to **[BAr$^F{}_4$]$^-$** anion signals give a ratio of **4.4: 1**.

Note: The ^{31}P{^{1}H} spectrum for 15 minutes coating was identical to that in Figure S3.

S.2.3. [1-NBA][BAr$^F{}_4$]@poly(ethylvinylether) – Solid-State NMR Characterization

Powdered samples of **[1-NBA][BAr$^F{}_4$]@poly(ethylvinylether)** (30 mgs) of material obtained after exposure to an EVE atmosphere for 30 seconds to EVE were packed in a 3.2 mm SS-NMR rotor, inside an argon filled glove box. The sample was immediately transferred to the bore of an 400MHz SS-NMR spectrometer and $^{31}P\{^1H\}$ and $^{13}C\{^1H\}$ Solid-State NMR spectra collected.

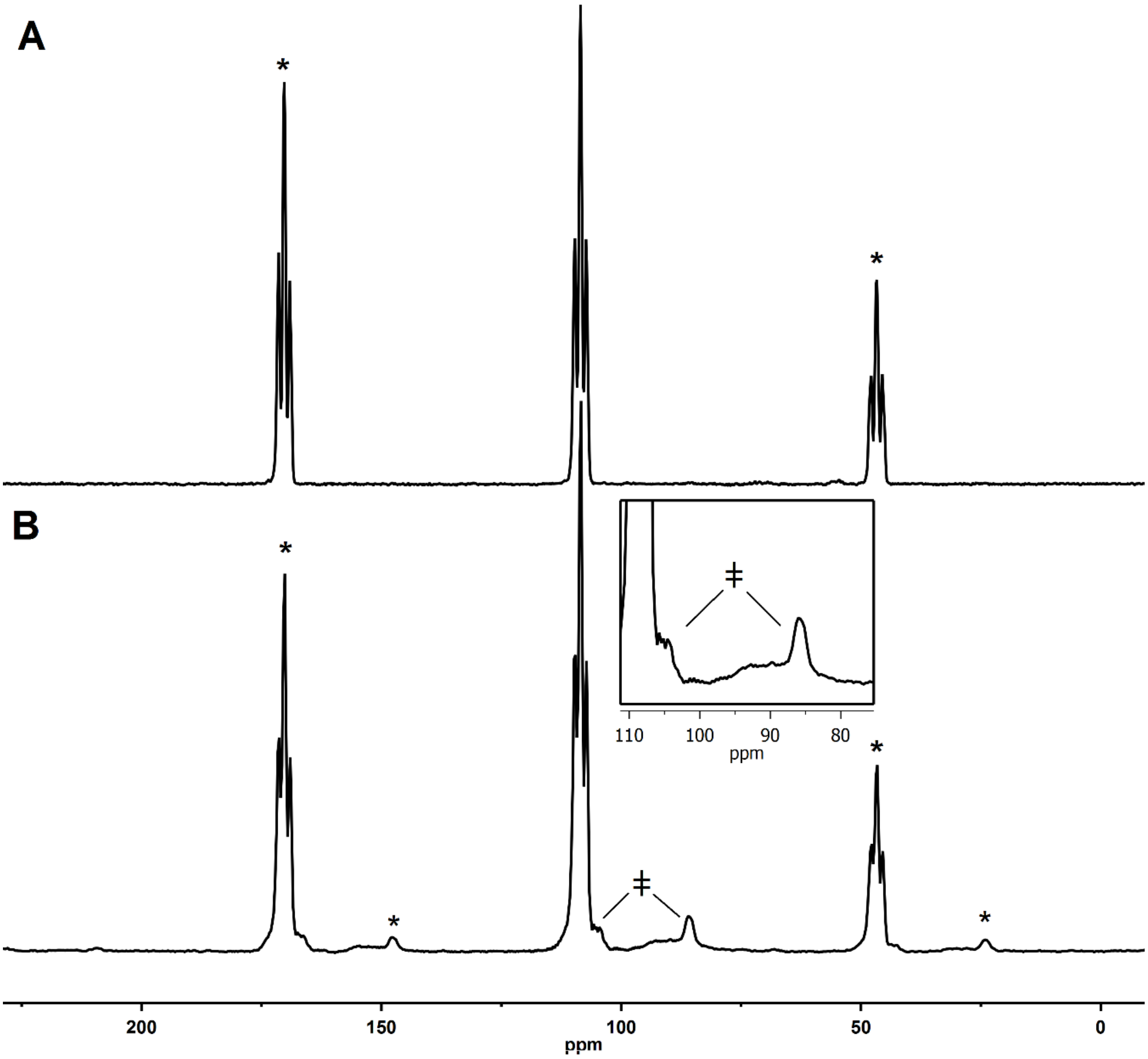

Figure S6: (A) The $^{31}P\{^1H\}$ SSNMR (162 MHz, 298 K, 10 kHz spin rate) spectrum of **[1-NBA][BAr$^F{}_4$]**.[S2] **(B)** The $^{31}P\{^1H\}$ SSNMR (162 MHz, 298 K, 10 kHz spin rate) spectrum of **[1-NBA][BAr$^F{}_4$]@poly(ethylvinylether).** The signal marked ‡ are possible ^{31}P environments associated with polymer-bound **[1-NBA][BAr$^F{}_4$]@poly(ethylvinylether)**. The resonances marked * are due to spinning sidebands. The inset is a zoom of the resonances between 110 and 85 ppm.

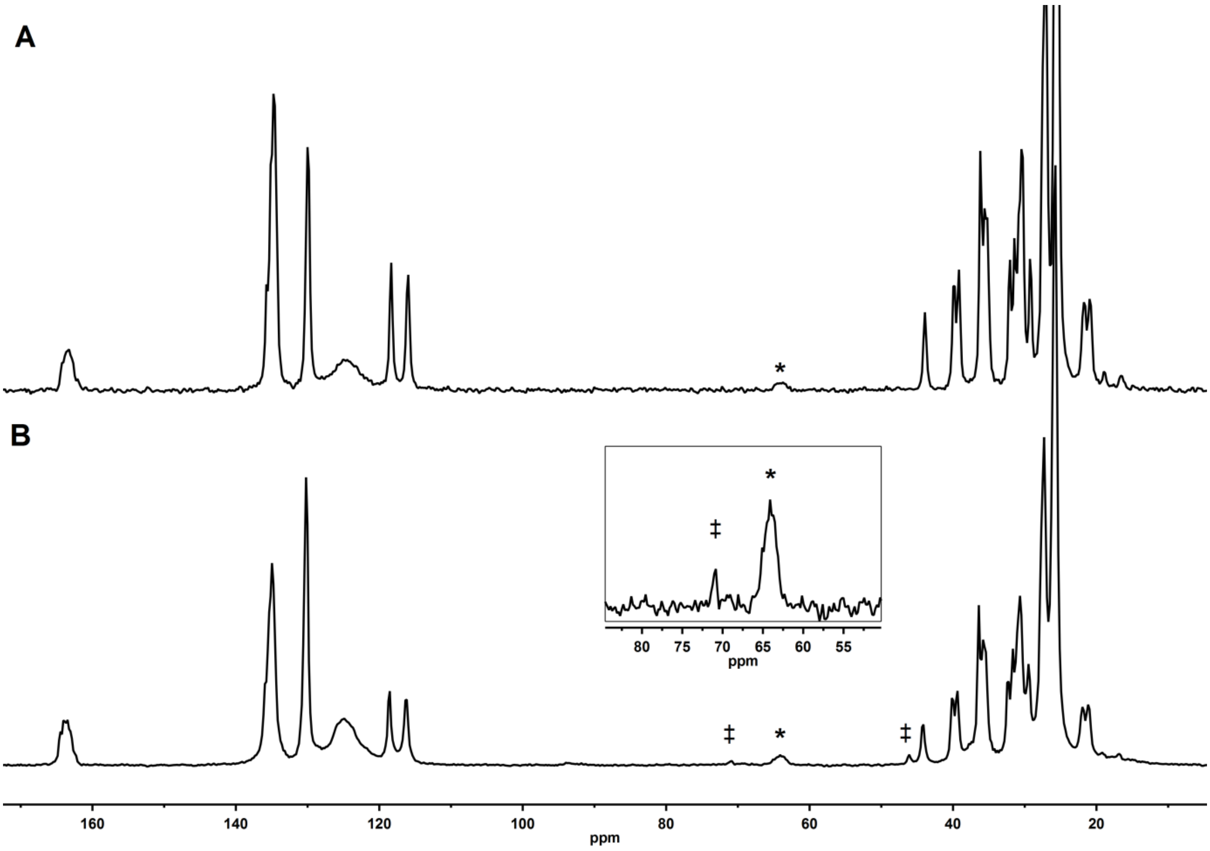

Figure S7: (A) The $^{13}C\{^1H\}$ SSNMR (100 MHz, 298 K, 10 kHz spin rate) spectrum of uncoated **[1-NBA][BAr$^F{}_4$]**.[S2] **(B)** The $^{13}C\{^1H\}$ SSNMR (100 MHz, 298 K, 10 kHz spin rate) spectrum of **[1-NBA][BAr$^F{}_4$]@poly(ethylvinylether)**.

The resonances marked ‡ at δ 71 and 44 are assigned to the ^{13}C environments of the coating polymer. The solution $^{13}C\{^1H\}$ NMR spectrum of neat **poly(ethylvinylether)** shows signals from -O**C**H$_2$- and –**C**H$_2$CH$_3$ at δ 74 and 42 respectively, see section S.4.2.[S4]

The resonances marked * are due to spinning sidebands. The inset is a zoom of the resonances between 90 and 50 ppm of **(B).**

S.2.4. [1-NBA][BAr$^{F}_{4}$]@poly(ethylvinylether) – A Single Crystal X-ray Diffraction Study

Single crystal x-ray diffraction was used to probe the change in crystallinity of **[1-NBA][BAr$^{F}_{4}$]@poly(ethylvinylether)** when the time of EVE exposure was varied.

Three separate batches of **[1-NBA][BAr$^{F}_{4}$]@poly(ethylvinylether)** (5 x crystals of approximately 1 x 1 x 1.5 mm in size and 1.0 mg mass per crystal) were prepared following the procedure in section S.2.1. The exposure time to an EVE atmosphere per batch was varied at 30 seconds, 2.5 minutes or 15 minutes. The samples were then were coated with Fomblin® Y oil under an argon-flush and a suitable crystal was rapidly selected and then transferred to the cryostream of a diffractometer and single-exposure frames at a range of angles were collected and a unit cell could be collected. From these frames the crystallinity of the sample was determined in a qualitative sense by the observation, or lack of, Bragg diffraction peaks. For 30 seconds exposure time to EVE, the crystals diffracted well, and a structure consistent with **[1-NBA][BAr$^{F}_{4}$]** could be solved and refined (R_1 = 7.5%).

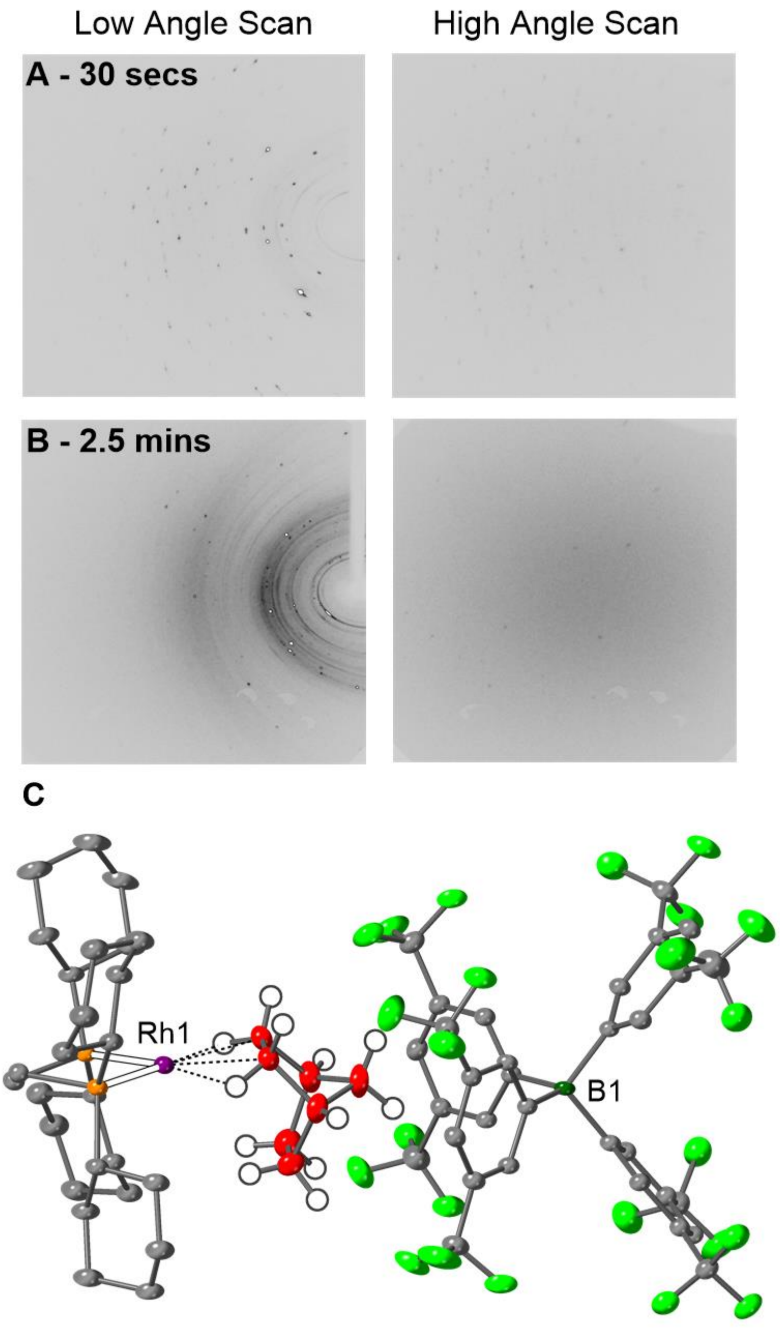

Figure S8: Example low and high angle single-exposure frames of crystalline **[1-NBA][BAr$^F{}_4$]@poly(ethylvinylether)** when exposed to an EVE atmosphere for **(A)** 30 seconds **(B)** 2.5 minutes. A unit cell could be found that matched **[1-NBA][BAr$^F{}_4$]**[S2] in collection **(A)** and **(B)**. After 15 minutes of **[1-NBA][BAr$^F{}_4$]** exposure to EVE, no Bragg peaks could be identified, suggesting no crystalline **[1-NBA][BAr$^F{}_4$]** remained. **(C)** Molecular structure of **[1-NBA][BAr$^F{}_4$]@poly(ethylvinylether)** with 30 seconds EVE exposure. Displacement ellipsoids set at 30% and hydrogen from phosphine ligand and [BAr$^F{}_4$]$^-$ anion removed for clarity in all parts.

S.2.5. [1-NBA][BAr$^F{}_4$]@poly(ethylvinylether) – SEM / EDX Images

Single crystal samples of **[1-NBD][BAr$^F{}_4$]**, **[1-NBA][BAr$^F{}_4$]** and **[1-NBA][BAr$^F{}_4$]@poly(ethylvinylether)** (the latter with EVE exposure times of 30 seconds, 2.5 minutes or 15 minutes) were prepared following the procedure in section S.2.1. All crystals used were of an approximate size of 1 x 1 x 1.5 mm and 1.0 mg in mass. These were then mounted upon carbon tape on stainless steel supports in an argon filled glove box and analysed by Scanning Electron Microscope (SEM) and Energy-Dispersive X-Ray (EDX).

Note: In all EDX composition images, small intensity signals can be seen for silicon. This was attributed to the grease used to help bind the crystals to the mounts, and not from polymer or rhodium complexes.

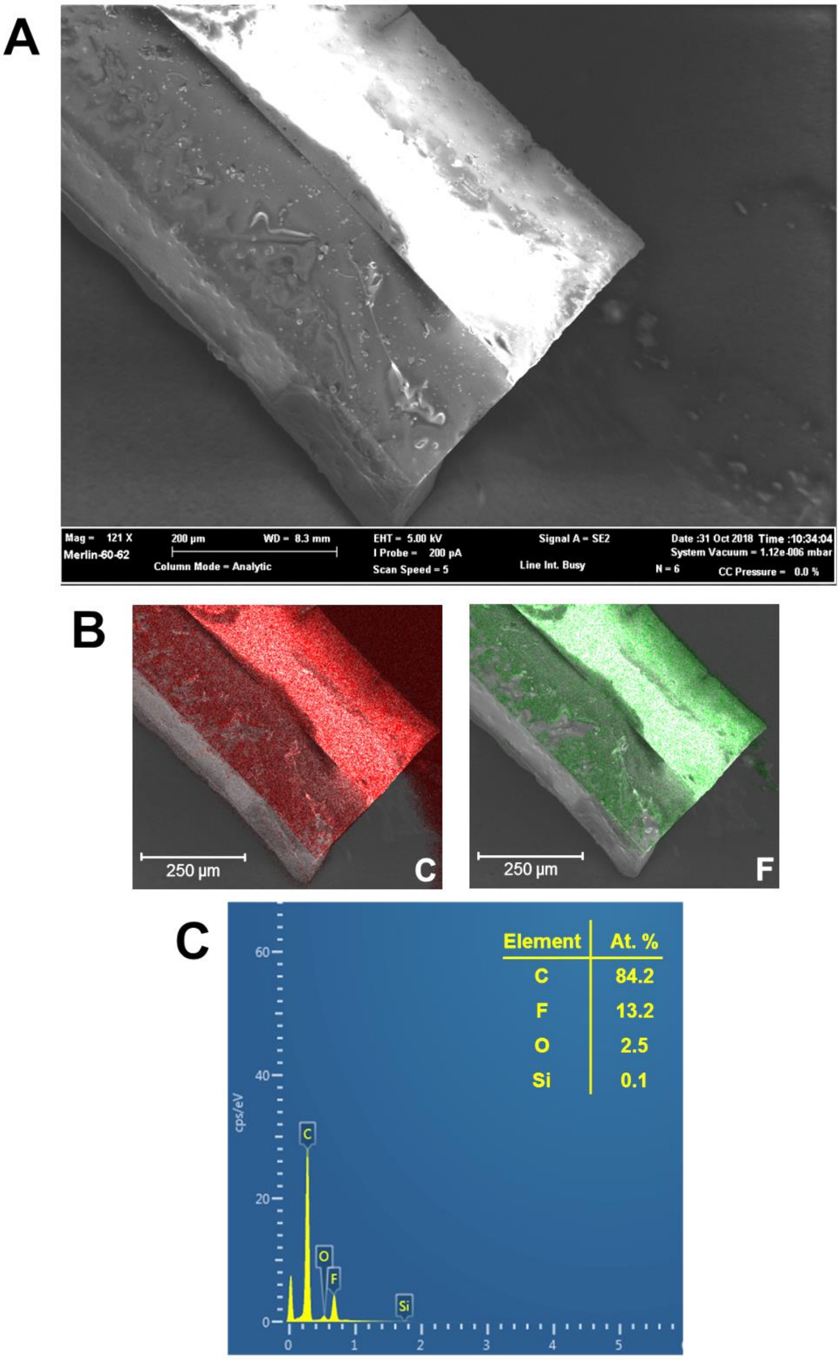

Figure S9: (A) SEM image of crystalline **[1-NBD][BAr$^F_4$]**. **(B)** EDX images of the same sample; with separate images showing intensity of individual elements coloured as follows: red = carbon and green = fluorine. **(C)** EDX sum spectrum of the sample with atomic percentage of the sample shown. Intense peaks for carbon and fluorine are attributed to the [BAr$^F_4$]$^-$ anion (**C: F** ratio is **6.4: 1** in this sample). No evidence could be seen for rhodium being present on the surface of the crystal.

Note: 2.5 At. % oxygen was measured. Although no polymer coating has been applied, and **[1-NBD][BAr$^F_4$]** contains no oxygen atoms, this signal is due to unavoidable contact with air when transferring the samples from argon filled glove box to vacuum of SEM machine.

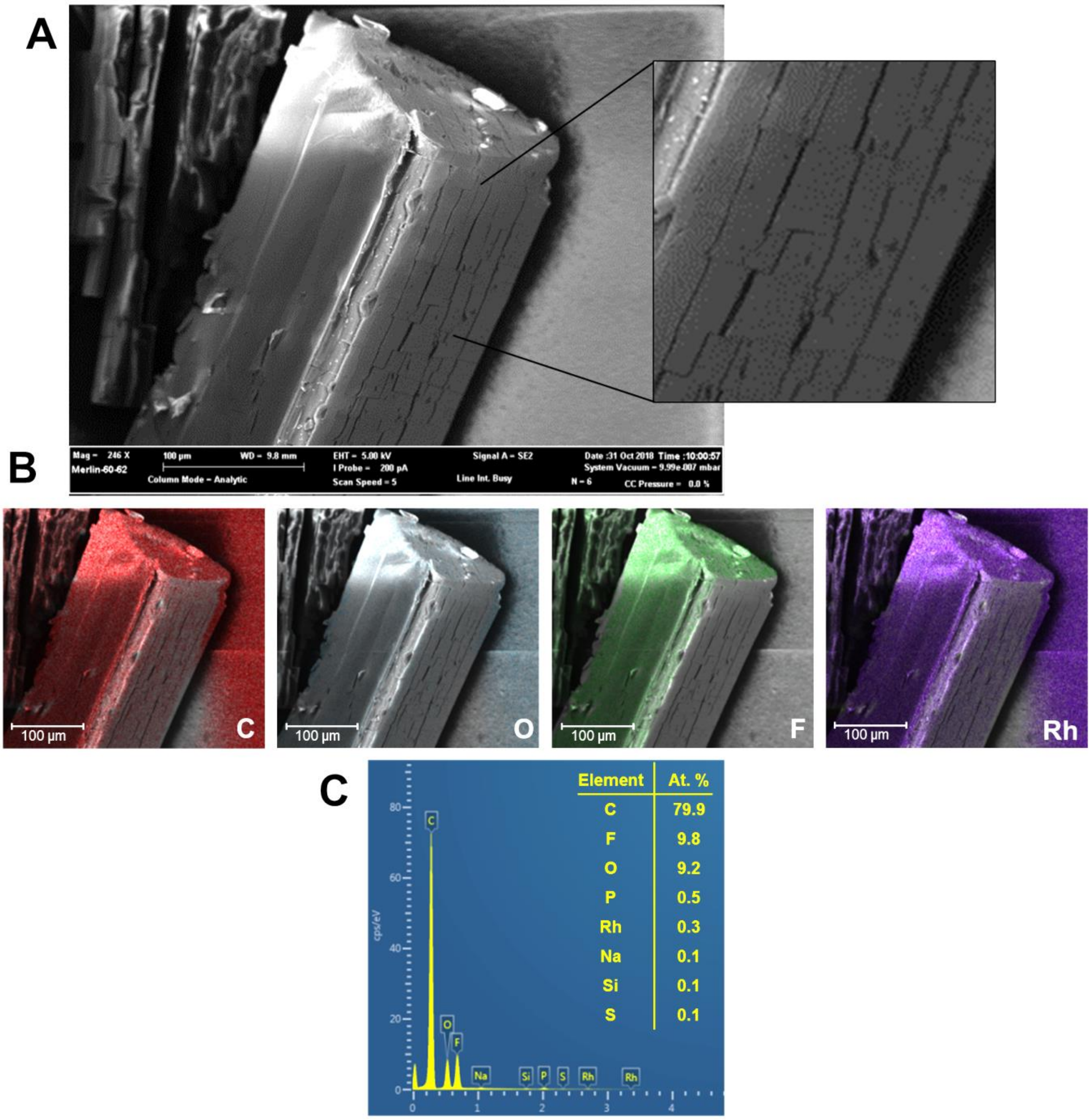

Element	At. %
C	79.9
F	9.8
O	9.2
P	0.5
Rh	0.3
Na	0.1
Si	0.1
S	0.1

Figure S10: (A) SEM image of crystalline **[1-NBA][BAr^F$_4$]** formed after 60 minutes of H_2 exposure to **[1-NBD][BAr^F$_4$]**. **(B)** EDX images of the same sample; with separate images showing intensity of individual elements coloured as follows: red = carbon, blue = oxygen, green = fluorine, purple = rhodium. **(C)** EDX sum spectrum of the sample with atomic percentage of the sample shown. Intense peaks for fluorine and carbon are attributed to the [BAr^F$_4$]$^-$ anion (**C: F** ratio is **8.1: 1** in this sample). Small, but significant levels of rhodium and phosphorus can now be seen, suggestive of micro-cracking of the crystalline surface during the hydrogenation reaction (Inset of figure S10A) exposing internal rhodium centres.

Note: 9.2 At. % oxygen was measured. Although no polymer coating has been applied, and **[1-NBA][BAr^F$_4$]** contains no oxygen atoms, this signal is due to unavoidable contact with air when transferring the samples from argon filled glove box to vacuum of SEM machine.

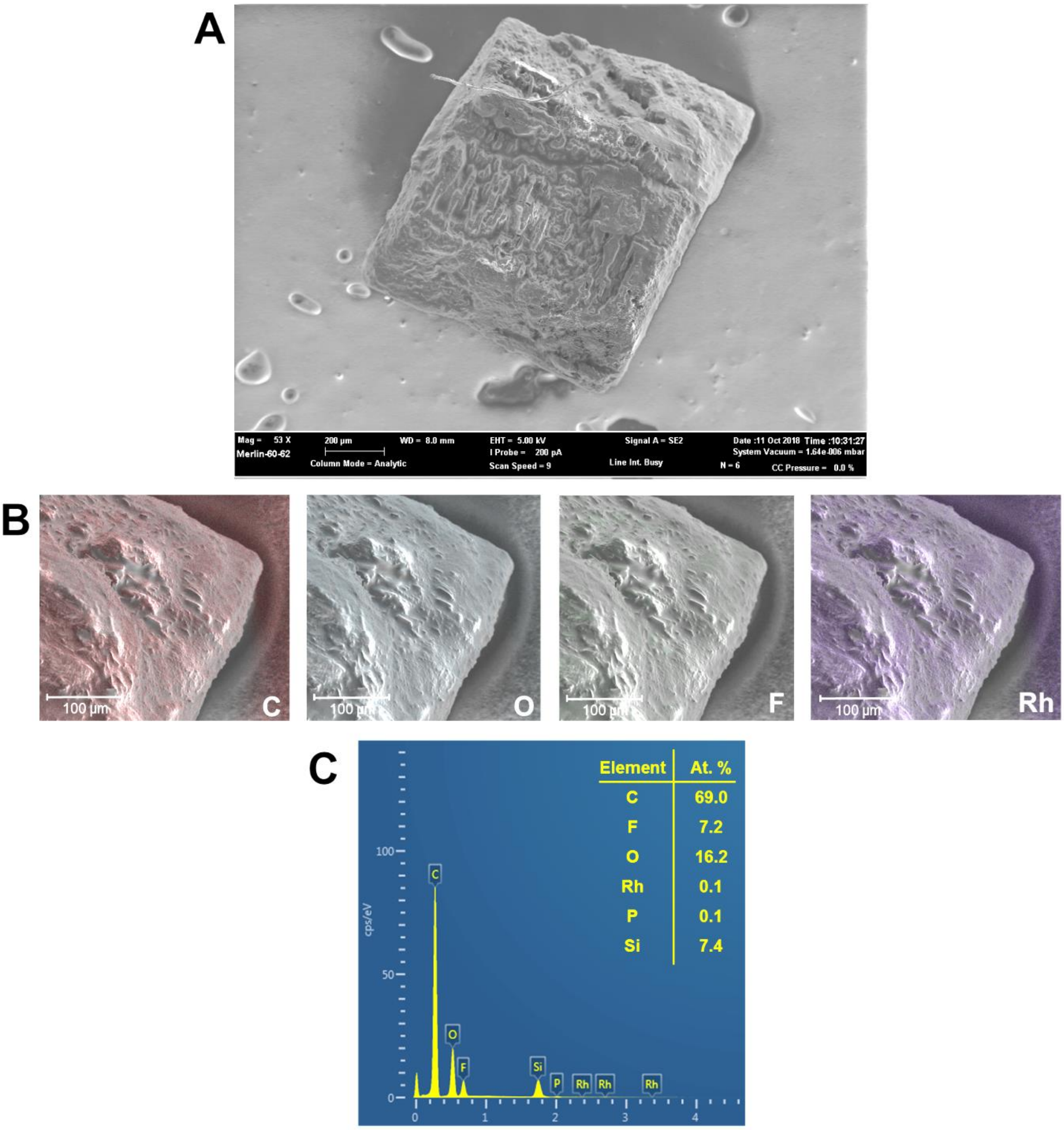

Figure S11: (A) SEM image of **[1-NBA][BAr$^F_4$]@poly(ethylvinylether)** which has been exposed to EVE for 30 seconds. **(B)** EDX images of the same sample; with separate images showing intensity of individual elements coloured as follows: red = carbon, blue = oxygen, green = fluorine, purple = rhodium. **(C)** EDX sum spectrum of the sample with atomic percentage of the sample shown, showing lower intensity peaks for fluorine, attributed to the [BAr$^F_4$]$^-$ anion, and exposed rhodium which has been partially covered in **poly(ethylvinylether)** (**C: F** ratio is **9.5: 1** in this sample). The increase in % oxygen is in line with **poly(ethylvinylether)** coating, where levels of oxygen have increased from 9.2 % to 16.2 % compared to **[1-NBA][BAr$^F_4$]**.

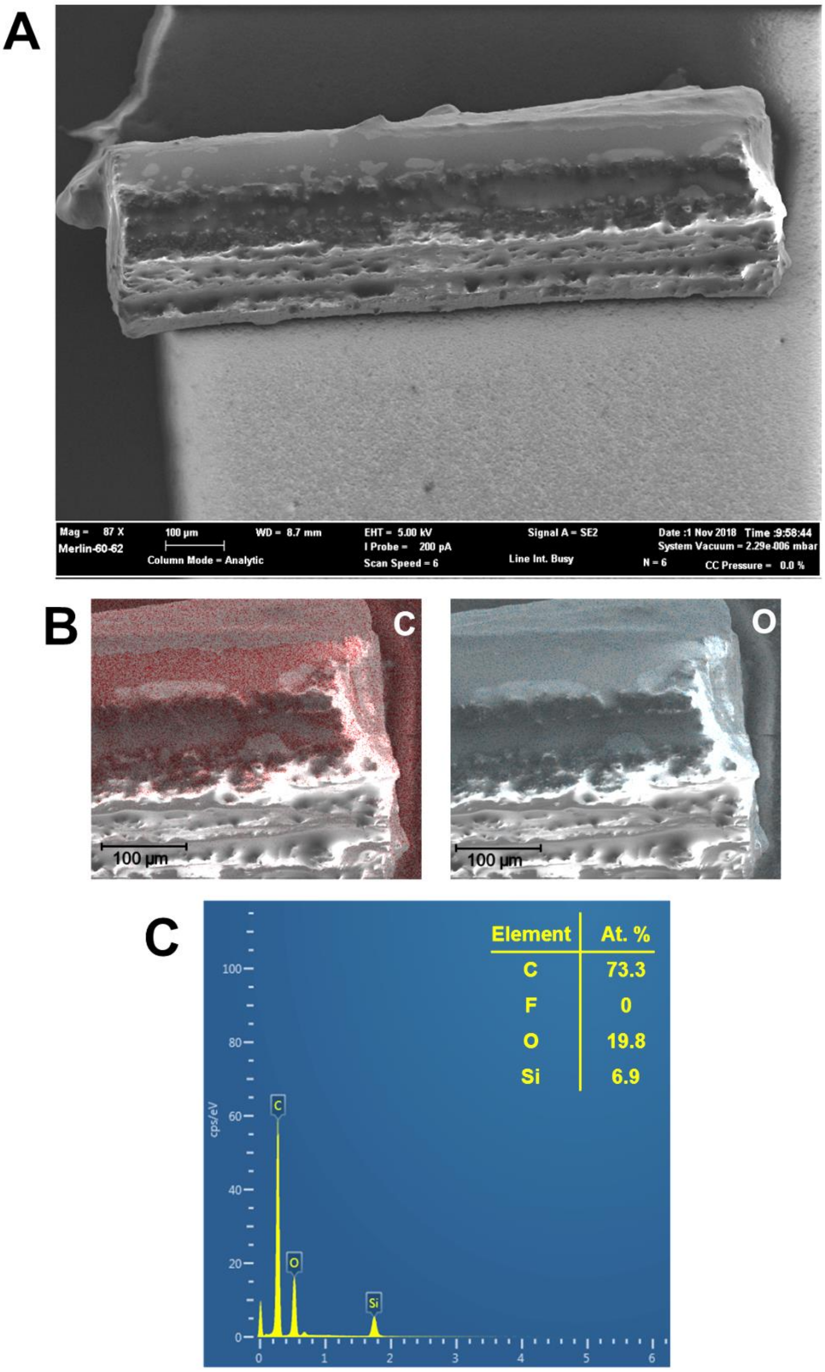

Figure S12: (A) SEM image of **[1-NBA][BAr$^F{}_4$]@poly(ethylvinylether)** which has been exposed to EVE for 2.5 minutes. **(B)** EDX images of the same sample; with separate images showing intensity of individual elements by coloured as follows: red = carbon, blue = oxygen. **(C)** EDX sum spectrum of the sample with atomic percentage of the sample shown, now showing no signals for fluorine or rhodium, suggesting full surface coverage of **poly(ethylvinylether)**. The intensity of oxygen has also increased again suggestive further **poly(ethylvinylether)** coverage. The crystals still retain structure, as shown by the well-defined ridges and corners.

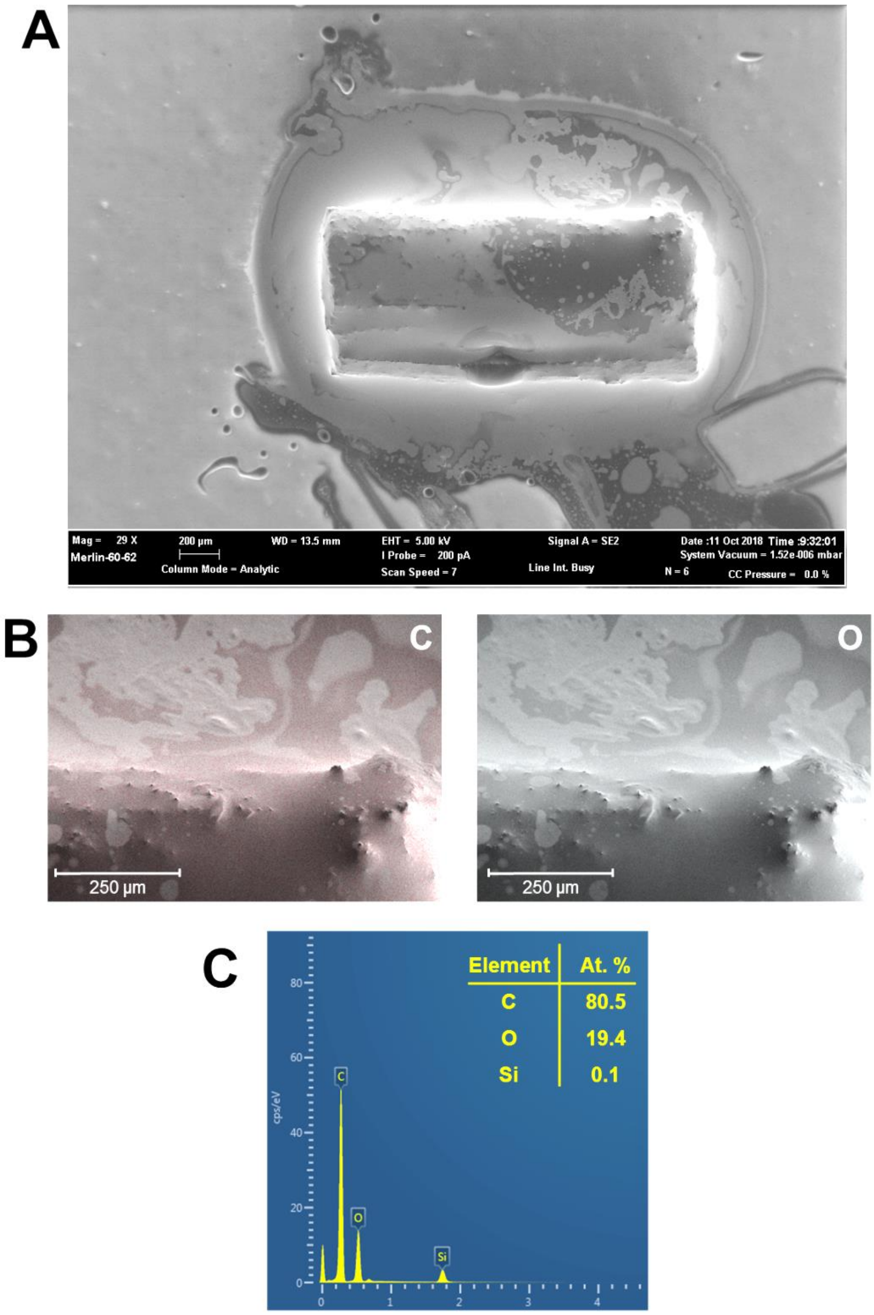

Element	At. %
C	80.5
O	19.4
Si	0.1

Figure S13: (A) SEM image of **[1-NBA][BAr$^F{}_4$]@poly(ethylvinylether)** which has been exposed to EVE for 15 minutes. **(B)** EDX images of the same sample; with separate images showing intensity of individual elements coloured as follows: red = carbon, blue = oxygen. **(C)** EDX sum spectrum of the sample with atomic percentage of the sample shown, which suggests no significant signals for fluorine or rhodium, suggesting full surface coverage of **poly(ethylvinylether)**. This is also shown by elemental atomic percentage present in **poly(ethylvinylether)** (carbon and oxygen) matching the calculated atomic percentage (At.%$_{calc}$ of ***poly*-EVE** = C: 80 %, O: 20 %).

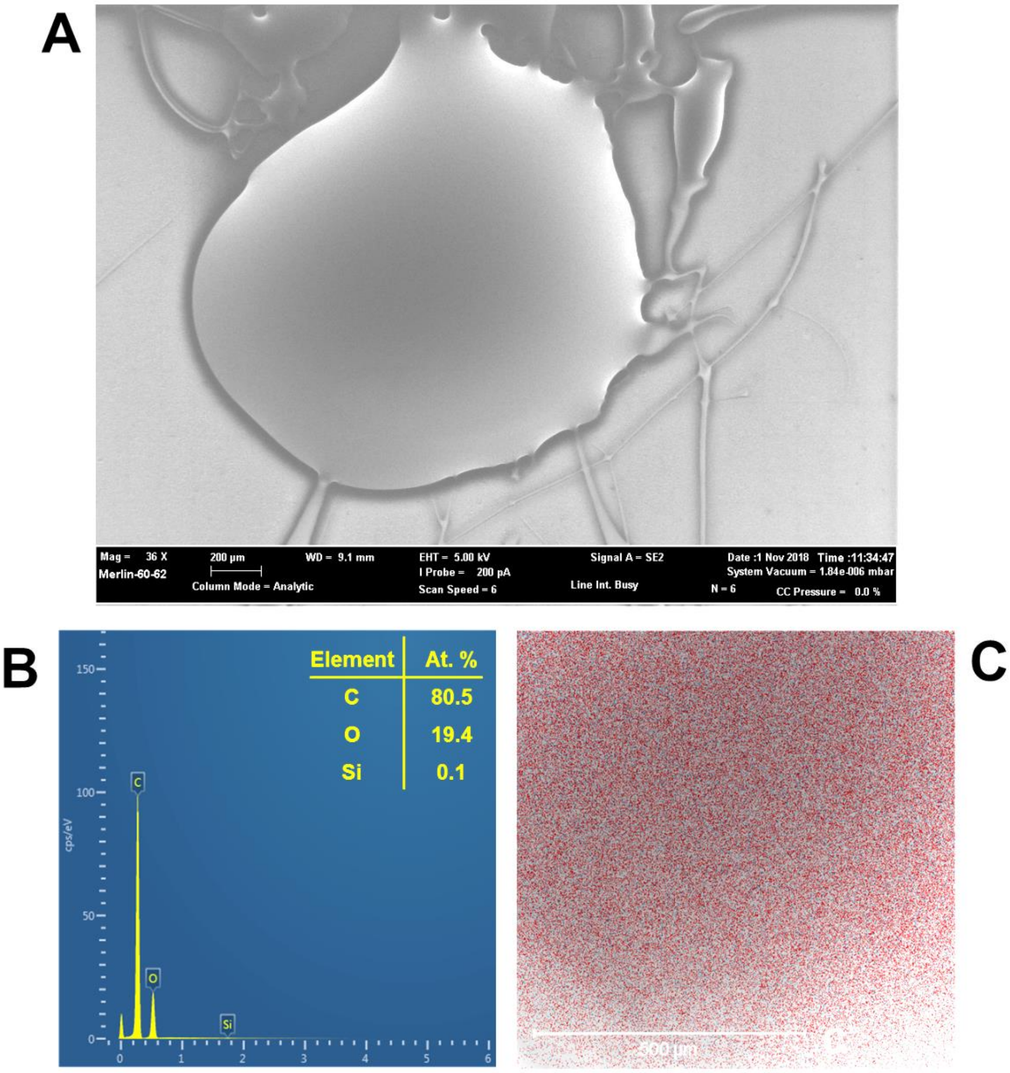

Element	At. %
C	80.5
O	19.4
Si	0.1

Figure S14: (A) SEM image of liquid **poly(ethylvinylether)**. **(B)** EDX sum spectrum of the sample with atomic percentage of the sample shown, showing just the presence of carbon and oxygen, corresponding to elements present in **poly(ethylvinylether)**, matching the calculated atomic percentage (At.%$_{calc}$ of **poly(ethylvinylether)** = C: 80 %, O: 20 %). **(C)** EDX element intensity images of the same sample; with separate images showing intensity of individual elements coloured as follows: red = carbon, blue = oxygen.

S.3. Experimental Procedures

S.3.1. Reactions of [1-NBA][BAr$^F_4$]@poly(ethylvinylether) with Air – A Single Crystal X-ray Diffraction Study

Single crystal x-ray diffraction could be used to probe the extent of crystallinity of **[1-NBA][BAr$^F_4$]@poly(ethylvinylether)** when exposed to air after 30 minutes, 2 and 8 hours.

[1-NBA][BAr$^F_4$]@poly(ethylvinylether) (crystals of approximately 1 x 1 x 1.5 mm in size and 1.0 mg in mass) were prepared following the procedure in section S.2.1., with 30 seconds EVE exposure time. The samples were then opened to air and left fully exposed whilst remaining on their mounts. After 30 mins, 2 hours and 8 hours air exposure, a suitable crystal was selected, coated with Fomblin® Y oil, transferred to the cryostream of a diffractometer and single-exposure frames at a range of angles were collected. From these frames the crystallinity of the sample was determined in a qualitative sense by the observation, or lack of, Bragg diffraction peaks.

Furthermore, the crystals with 30 seconds EVE exposure and then 30 minutes air exposure had a full dataset collected, which could be solved and refined to match that of **[1-NBA][BAr$^F_4$]**.[S2] The crystal structure is shown in Figure S16.

If not coated in the protective polymer layer, the dark red **[1-NBA][BAr$^F_4$]** rapidly reacts with air to give the green crystals, see section S.3.2.

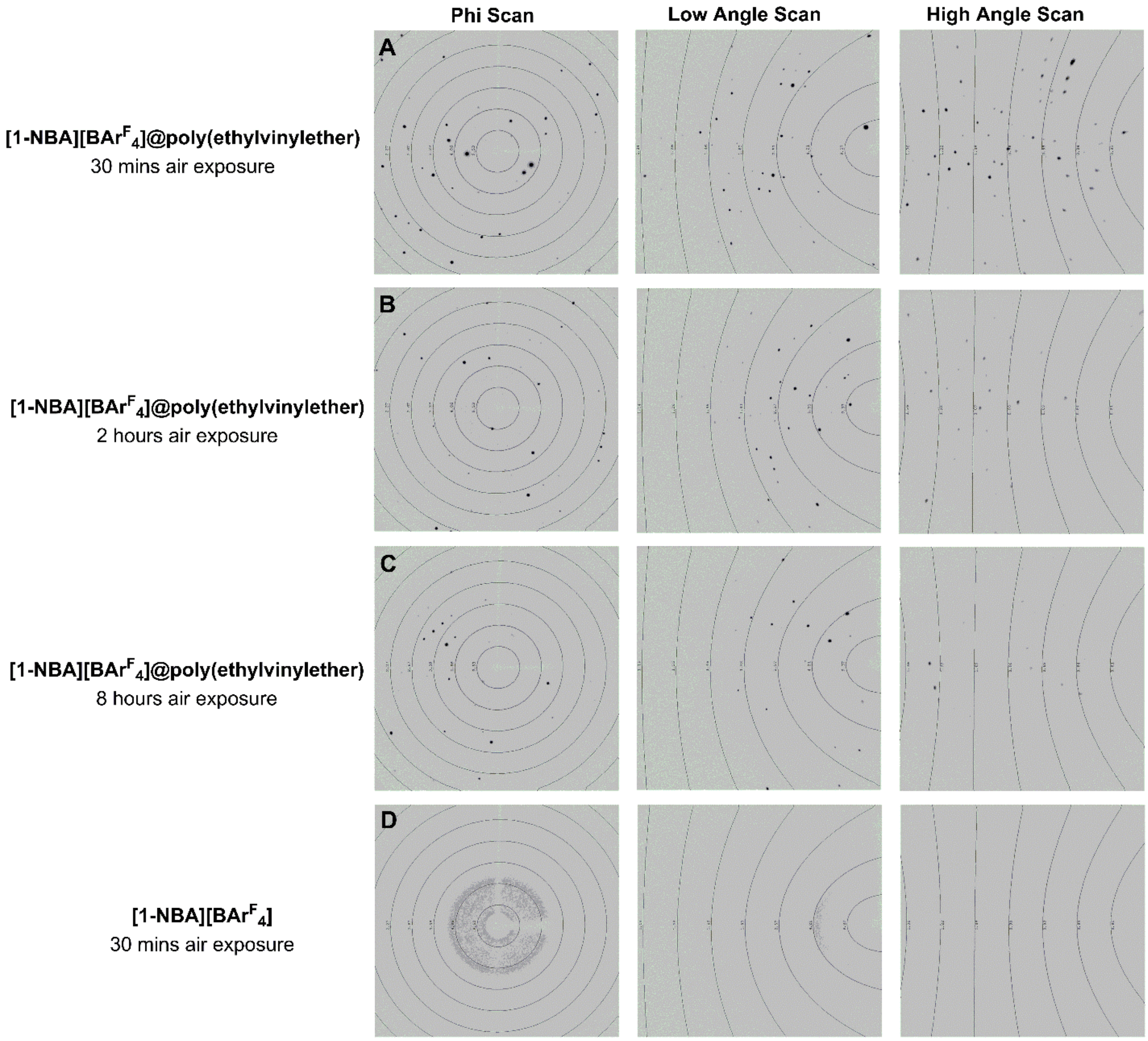

Figure S15: Example single frames of a Phi, Low and High angle scan of crystalline **[1-NBA][BAr$^F_4$]@poly(ethylvinylether)** (30 seconds exposure to an EVE atmosphere) when exposed to an air for **(A)** 30 minutes **(B)** 2 hours **(C)** 8 hours. These spots could all be indexed to the unit cell of **[1-NBA][BAr$^F_4$]**.[S2] **(D)** Example frames of **[1-NBA][BAr$^F_4$]** which has been exposed to air for 30 minutes. No spots could be located suggesting no long-range crystallinity.

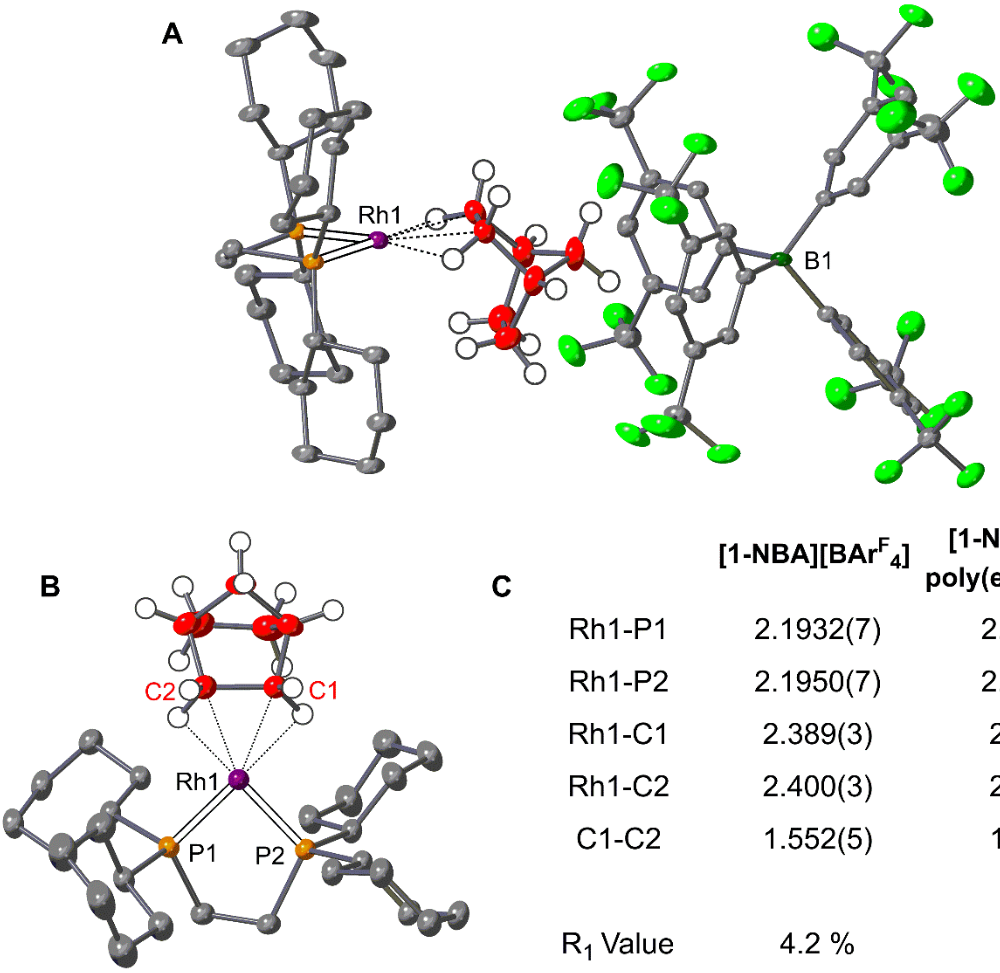

C

	[1-NBA][BAr$^F_4$]	**[1-NBA][BAr$^F_4$]@ poly(ethylvinylether)**
Rh1-P1	2.1932(7)	2.1854(7)
Rh1-P2	2.1950(7)	2.1949(7)
Rh1-C1	2.389(3)	2.389(3)
Rh1-C2	2.400(3)	2.409(3)
C1-C2	1.552(5)	1.544(5)
R_1 Value	4.2 %	4.9 %

Figure S16: **(A)** Molecular structure of **[1-NBA][BAr$^F_4$]@poly(ethylvinylether)** (30 seconds EVE exposure) after being exposed to air for 30 minutes. **(B)** Enlarged view of the isolated cation. **(C)** Table shows selected bond metrics of **[1-NBA][BAr$^F_4$]**[S2] versus **[1-NBA][BAr$^F_4$]@poly(ethylvinylether)**. Displacement ellipsoids set at 30% and hydrogen from phosphine ligand and [BAr$^F_4$]$^-$ anion removed for clarity in all parts.

S.3.2. Reactions of [**1-NBA][BAr$^F{}_4$]@poly(ethylvinylether)** with Air – Optical Images

As well as using single crystal x-ray diffraction analysis, optical images were taken to highlight the relative rates of decomposition when **[1-NBA][BAr$^F{}_4$]** and **[1-NBA][BAr$^F{}_4$]@poly(ethylvinylether)** are left exposed to air.

Crystals of **[1-NBA][BAr$^F{}_4$]** and **[1-NBA][BAr$^F{}_4$]@poly(ethylvinylether)** (30 seconds exposure to an EVE atmosphere) were placed on a microscope slide within an argon filled glove box with graphing paper placed behind. They were rapidly transferred to a microscope with camera set-up outside the glove box in air; where photos could be taken at periodic time intervals (1, 5, 30 minutes and 8, 24, 72 hours).

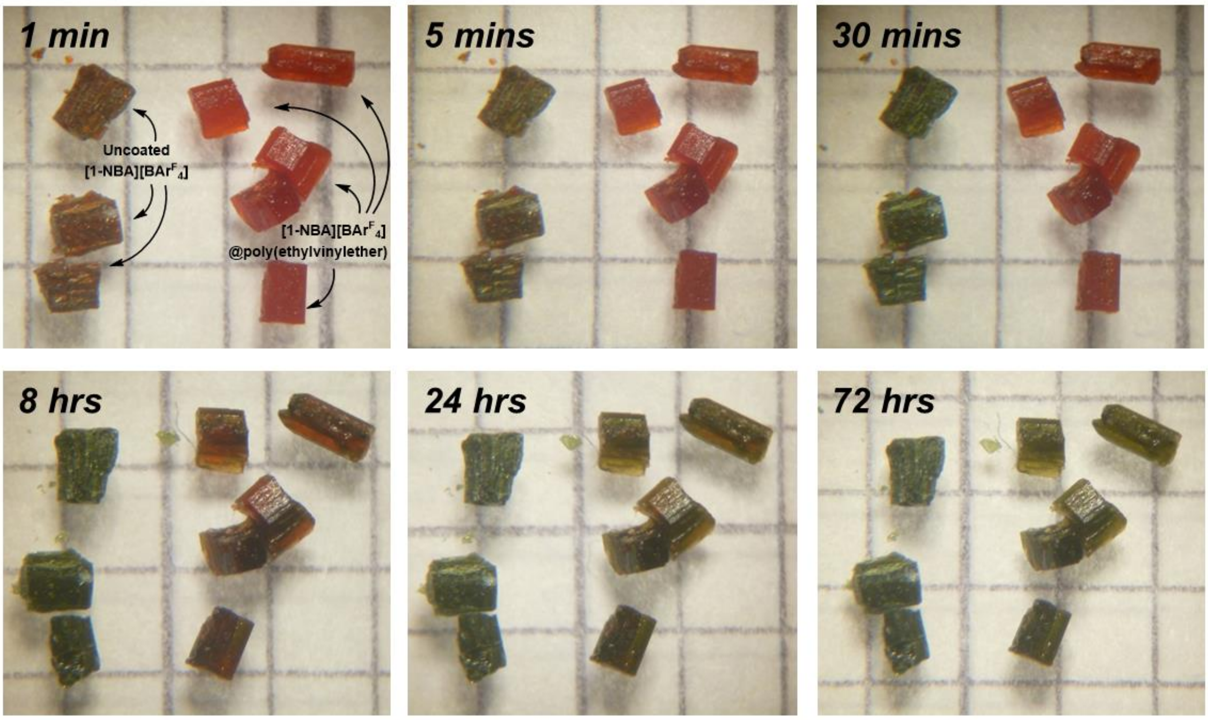

Figure S17: Optical images of samples of **[1-NBA][BAr$^F{}_4$]** and **[1-NBA][BAr$^F{}_4$]@poly(ethylvinylether)** left in air. The photos were taken after 1, 5, 30 minutes and 8, 24, 72 hours. Each grid marks 2 mm x 2 mm.

Clear differentiation of the two samples at 30 minutes air-exposure can be seen, where the green coloured, un-coated, air reacted product is shown next to the dark red crystals of air tolerant **[1-NBA][BAr$^F{}_4$]@poly(ethylvinylether)**.

Due to the very reactive nature of **[1-NBA][BAr^F$_4$]**, even at time-of-measuring (1 min) some colour change can be seen. When under an argon atmosphere **[1-NBA][BAr^F$_4$]** is a dark-red colour.

In uncoated samples of **[1-NBA][BAr^F$_4$]** the crystals turned light green in colour after 30 mins, which took 72 hours for **[1-NBA][BAr^F$_4$]@poly(ethylvinylether)**. This green complex was amorphous in nature, so could not be analysed by single crystal x-ray diffraction, but could be analysed by solid-state NMR spectroscopy (Figure S18). Unfortunately, the precise nature of these complexes could not be unambiguously identified by either solution or solid-state NMR spectroscopy.

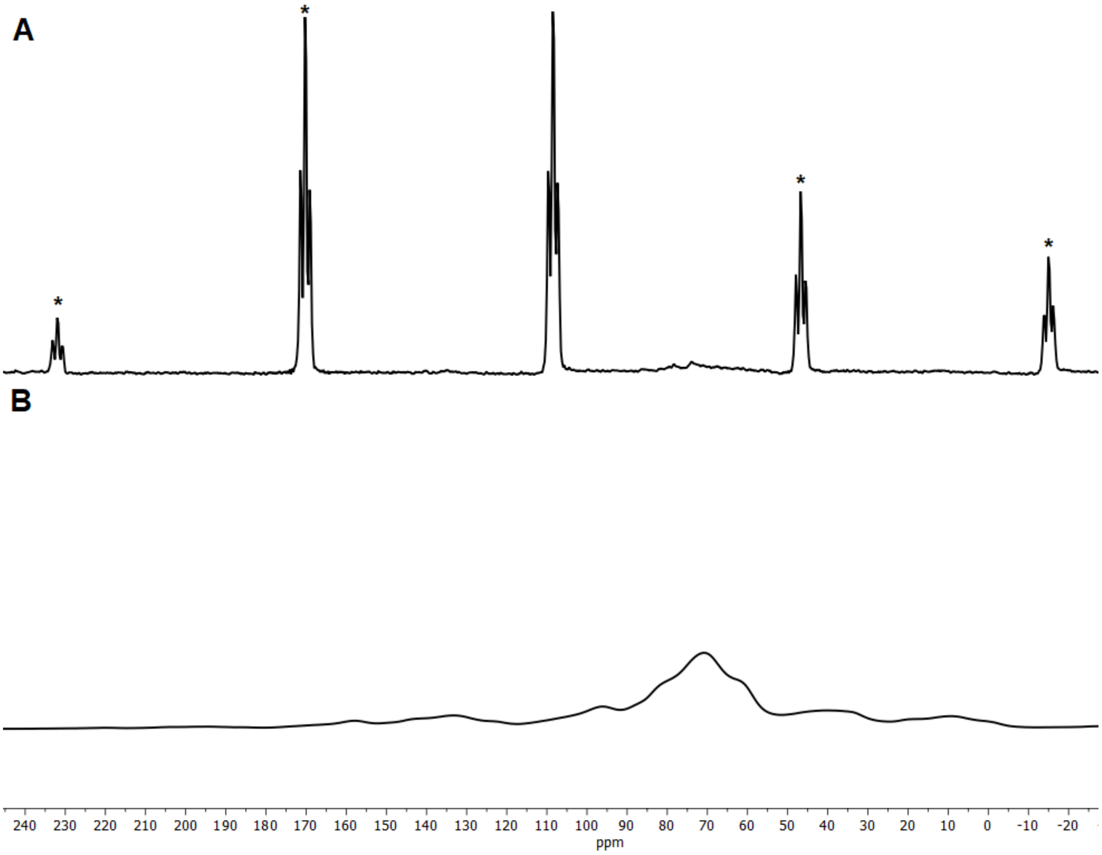

Figure S18: The $^{31}P\{^1H\}$ SSNMR (162 MHz, 298 K, 10 kHz spin rate) spectrum of **(A) [1-NBA][BAr^F$_4$]@poly(ethylvinylether)** after 30 seconds EVE exposure and 30 minutes air exposure. **(B)** Not coated, **[1-NBA][BAr^F$_4$]** exposed to air for 30 minutes, (FWHM = 4200 Hz). Peaks marked * are spinning sidebands.

We note the broad, low intensity features between δ 105 and 80 present in the spectrum of **[1-NBA][BAr^F$_4$]@poly(ethylvinylether)** (Figure S6) are no longer present. Whether this is due to surface located species undergoing reactions with oxygen is not clear.

S.3.3. Reactions of [1-NBA][BAr$^F_4$]@poly(ethylvinylether) with Propene Gas

[1-NBA][BAr$^F_4$]@poly(ethylvinylether) (crystals of approximately 1 x 1 x 1.5 mm in size and 1.0 mg in mass) were prepared following the procedure in section S.2.1., with 30 seconds EVE exposure time. The flask was placed under vacuum (< 3 × 10^{-2} mbar) and propene (1 bar, 298 K) was added. After 5 days, the flasks was evacuated and re-filled with argon, to yield yellow/orange crystals of $[Rh(Cy_2PCH_2CH_2PCy_2)(C_3H_6)][BAr^F_4])$@poly(ethylvinylether), **[1-C_3H_6][BAr$^F_4$]@poly(ethylvinylether)**.

When dissolved in CD_2Cl_2 and analysed by solution ^{1}H and ^{31}P{^{1}H} NMR spectroscopy, or analysed directly by solid-state ^{31}P{^{1}H} and ^{13}C{^{1}H} NMR spectroscopy and single-crystal x-ray diffraction showed the formation to **[1-C_3H_6][BAr$^F_4$]@poly(ethylvinylether)**. Further information about the single-crystal x-ray diffraction refinement structure can be found in section S.6.

^{31}P{^{1}H} solution NMR (CD_2Cl_2, 126 MHz, 298 K) δ: 95.1 (br d, J_{RhP} = 180 Hz). (Reported value of δ 95.2 (br d, J_{RhP} = 181 Hz)).[S5]

^{31}P{^{1}H} SSNMR (162 MHz, 10 kHz spin rate, 298 K): δ 95.3 (br s.). (Reported value of δ 95.6 (br s.).[S5]

^{1}H solution NMR (CD_2Cl_2, 400 MHz, 298 K) δ: 7.71 (8H, s, BAr$^F_4$), 7.54 (4H, s, BAr$^F_4$), ~ 5.1 (br, propene), 2.02-0.94 (~ 60H, multiple overlapping aliphatic resonances).[S5]

Note: On a separate batch to that above **[1-NBA][BAr$^F_4$]@poly(ethylvinylether)** was left under propene for 2 days. When analysed by solution ^{31}P{^{1}H} NMR spectroscopy after this time, two complexes were observed in approximate 50:50 ratio of **[1-C_3H_6][BAr$^F_4$]@poly(ethylvinylether)** and **[1-BAr$^F_4$]**, where **[1-BAr$^F_4$]** is the product of decomposition of **[1-NBA][BAr$^F_4$]** in solution.[S2] After 2 hours under a propene atmosphere, un-coated **[1-NBA][BAr$^F_4$]** was fully converted to **[1-C_3H_6][BAr$^F_4$]**.

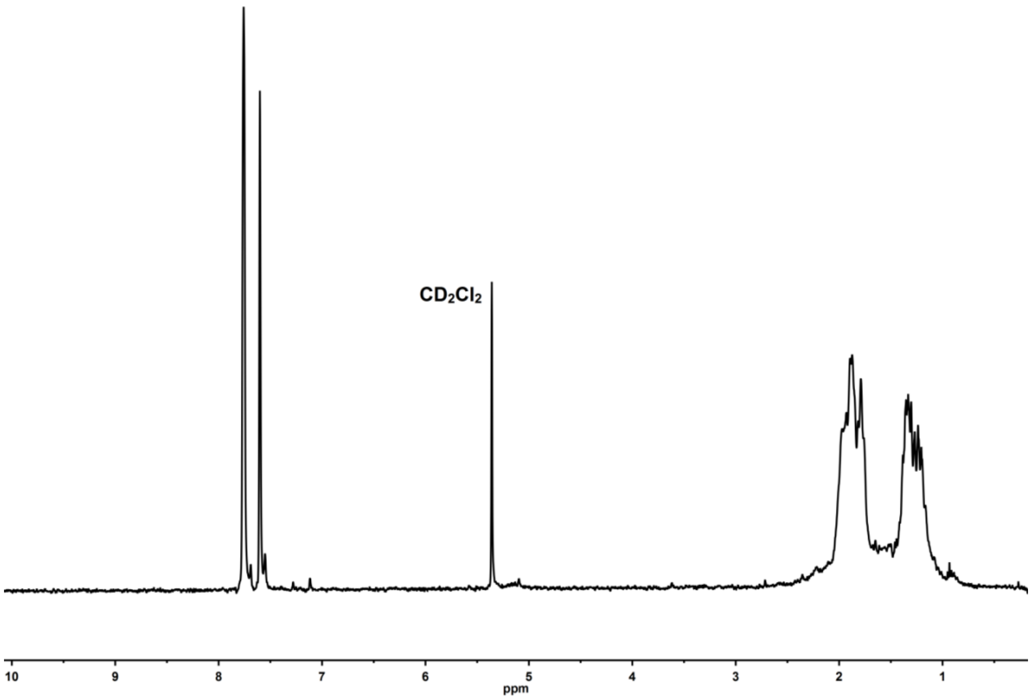

Figure S19: The solution ^{1}H NMR (CH$_2$Cl$_2$, 298 K, 400 MHz) spectrum of **[1-C$_3$H$_6$][BAr^F$_4$]@poly(ethylvinylether)**, equivalent to previously reported **[1-C$_3$H$_6$][BAr^F$_4$].**^{S5}

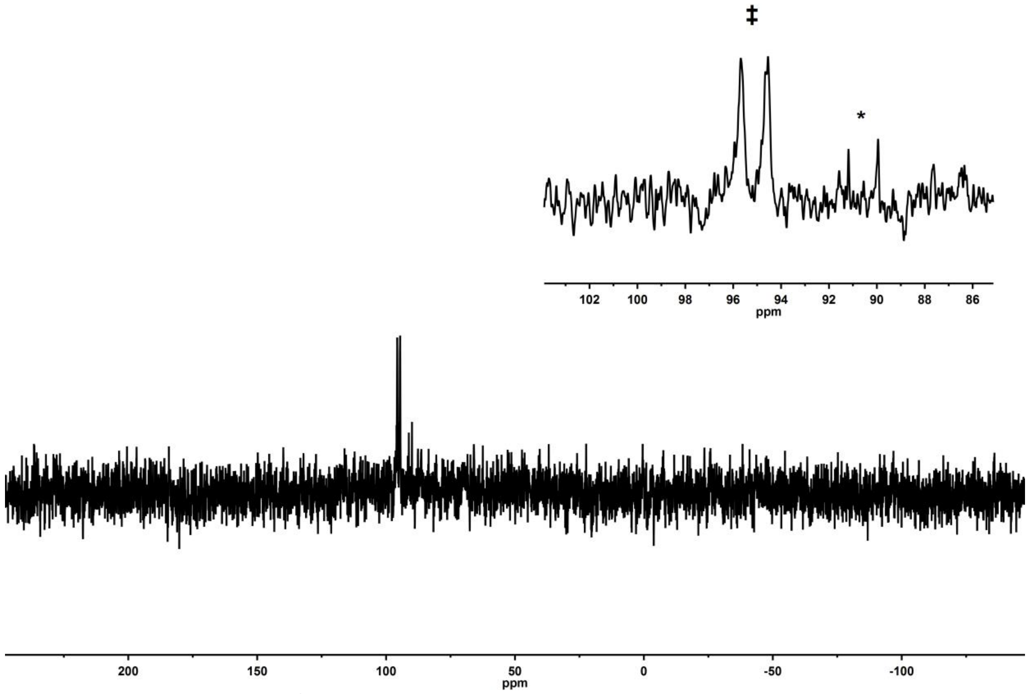

Figure S20: The solution ^{31}P{^{1}H} NMR (CH$_2$Cl$_2$, 298 K, 126 MHz) spectrum of **[1-C$_3$H$_6$][BAr^F$_4$]@poly(ethylvinylether)**, equivalent to previously reported **[1-C$_3$H$_6$][BAr^F$_4$].**^{S5}

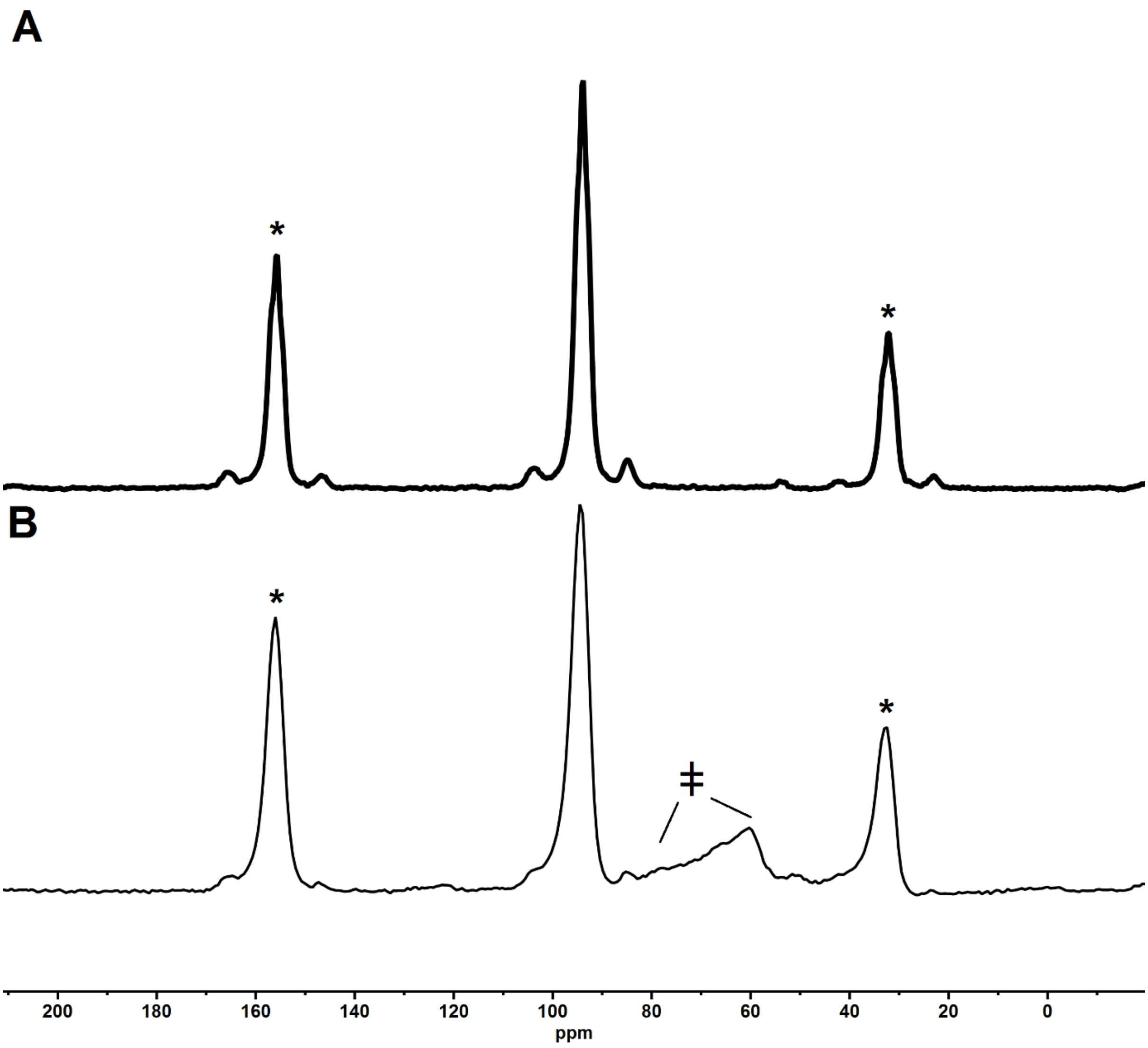

Figure S21: (A) The previously reported $^{31}P\{^{1}H\}$ SSNMR (162 MHz, 298 K, 10 kHz spin rate) spectrum of **[1-C_3H_6][BAr$^F{}_4$]**.[S5] **(B)** The $^{31}P\{^{1}H\}$ SSNMR (162 MHz, 298 K, 10 kHz spin rate) spectrum of **[1-C_3H_6][BAr$^F{}_4$]@poly(ethylvinylether)**.

The signals marked ‡ are possible ^{31}P environments associated with polymer-bound **[1-C_3H_6][BAr$^F{}_4$]@poly(ethylvinylether)**. The resonances marked ***** are due to spinning sidebands.

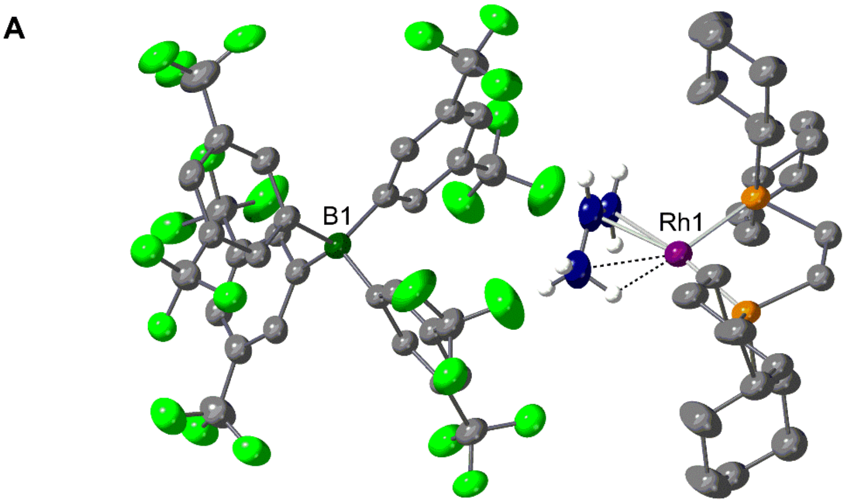

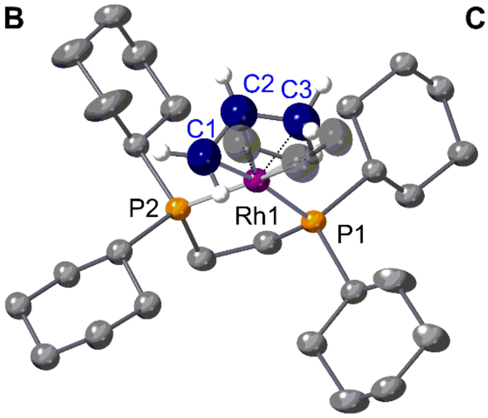

C

	$[1\text{-}C_3H_6][BAr^F_4]$	$[1\text{-}C_3H_6][BAr^F_4]$@poly(ethylvinylether)
Rh1-P1	2.235(3)	2.232(2)
Rh1-P2	2.240(3)	2.238(2)
Rh1-C1	2.24(2)	2.259(16)
Rh1-C2	2.15(2)	2.18(2)
Rh1-C3	2.29(2)	2.33(2)
C1-C2	1.24(3)	1.28(3)
C2-C3	1.36(3)	1.40(3)
R_1 Value	12.77 %	10.03 %

Figure S22: **(A)** Molecular structure of **$[1\text{-}C_3H_6][BAr^F_4]$@poly(ethylvinylether)** with 30 seconds EVE exposure. **(B)** Enlarged view of the isolated cation, disorder component of the propene ligand shown in translucent grey. **(C)** Table shows selected bond metrics and refinement data of **$[1\text{-}C_3H_6][BAr^F_4]$**[S5] versus **$[1\text{-}C_3H_6][BAr^F_4]$@poly(ethylvinylether)**. Displacement ellipsoids set at 30% and hydrogen atoms from phosphine ligand and $[BAr^F_4]^-$ anion removed for clarity in all parts.

S.4. Catalytic Polymerisation Experiments in Bulk

S.4.1. Catalytic Solid-Vapour Polymerisation Procedures

Method A

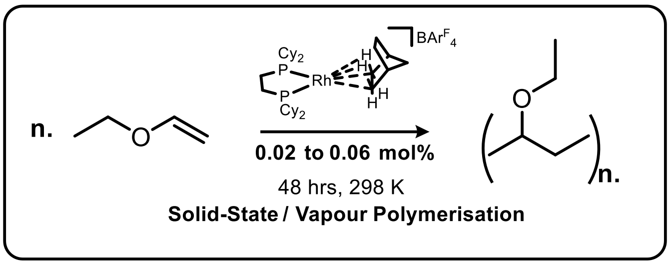

To Mount: Inside an argon filled glove box, crystal(s) of **[1-NBD][BAr^F$_4$]** were affixed to the side wall of a J. Young flask with aid of a small amount of silicon grease, as shown in Figure S25. The number of **[1-NBD][BAr^F$_4$]** crystals and approximate size / mass varied on experimental procedure, see Table S1 / Figure S28. A glass insert made from a sealed Pasteur pipette (see section S.5.1.) was also placed inside the flask.

Once mounted: The J. Young flask (~ 50 mL) was sealed and evacuated (< 3 × 10^{-2} mbar), filled with H_2 gas (15 psi, 298 K) and left to stand for 30 mins, to form **[1-NBA][BAr^F$_4$]** *in situ*. Care was taken to not dislodge any mounted crystals during gas evacuation / addition.

After this time, H_2 was removed under vacuum (< 3 × 10^{-2} mbar) and placed under an argon atmosphere. Ethyl Vinyl Ether (EVE) (0.15 mL) was then syringed into the insert within the flask. The flask was sealed and stored upright, to which the volatile nature of EVE allowed for a vapour atmosphere to be formed, as a timer was started.

Within 1 hour, a stream of liquid polymer can be visibly seen flowing down from the affixed crystal, so that the polymer starts to pool at the bottom of the flask, and not flow into the monomer containing insert. The reaction was then left until polymer flow had stopped (~ 48 hours); suggestive of complete monomer consumption, at which point the flask was then opened to air, and the resulting polymer extracted into CH_2Cl_2 (3 x 10 mL). After drying *in vacuo* overnight, the polymer was characterised as **poly(ethylvinylether)** by ^{1}H and ^{13}C{^{1}H} NMR spectroscopy and GPC analysis.

Note: The glass insert was necessary as to separate monomer and flowing polymer. If not, the monomer dissolves in polymer pool. Not all liquid EVE vaporises instantly, unlike in section S.2.1., as excess of x 1000 of EVE is used.

The above procedure was repeated numerous times, varying total mass and total surface area of **[1-NBA][BAr$^F{}_4$]** initiator. The initiator loading studies were performed by picking single crystals of the same approximate size and mass (total crystal masses of 0.5, 1.0 and 1.5 mg with approximate sizes of 0.5 x 0.5 x 1.0 mm, 1.0 x 1.0 x 1.5 mm and 1.0 x 2.0 x 2.0 mm respectively) to 0.15 mL of EVE. Further to this; an experiment made up of loading 3 x crystals of 0.5 mg with approximate sizes 0.5 x 0.5 x 1.0 mm each; where all 3 were loaded in one reaction, directly probing surface area effects. Thus, the total initiator mass is 1.5 mg. This is directly comparable to the reaction of one crystal of 1.5 mg, where the surface area of active initiator has now been increased ~ 3 times. Each experiment was repeated three times and averages plotted in Table S1 / Figure S28.

^{1}H NMR of **poly(ethylvinylether)** (CD_2Cl_2, 400 MHz, 183 K): δ 3.53 (br s, 1H, -OC**H**-), 3.43 (br, 2H, -OC**H$_2$**-), 1.90-1.37 (m, 2H, -C**H$_2$**-), 1.13 (br, 3H, -C**H$_3$**)

^{13}C{^{1}H} NMR of **poly(ethylvinylether)** (CD_2Cl_2, 100 MHz, 298K): δ 74 - 73 (br m, -O**C**H$_2$-), 65 – 63 (br m, -O**C**H-), 42 -39 (m, -**C**H$_2$-), 15.7 (m, -**C**H$_3$).

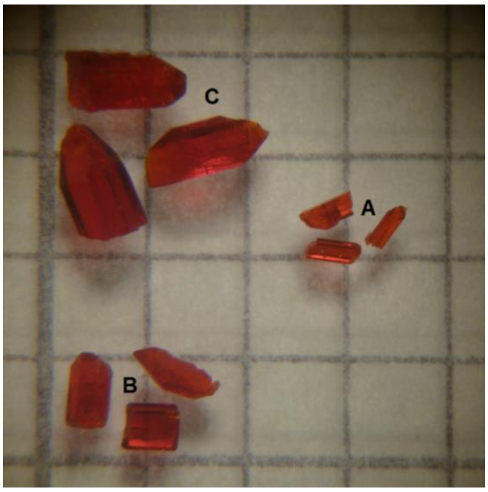

Figure S23: Example images of the crystals of **[1-NBD][BAr$^F{}_4$]** used in the solid-vapor polymerization reactions, where **(A)** 0.5 mg **(B)** 1.0 mg and **(C)** 1.5 mg. Grid scale = 2 mm x 2 mm.

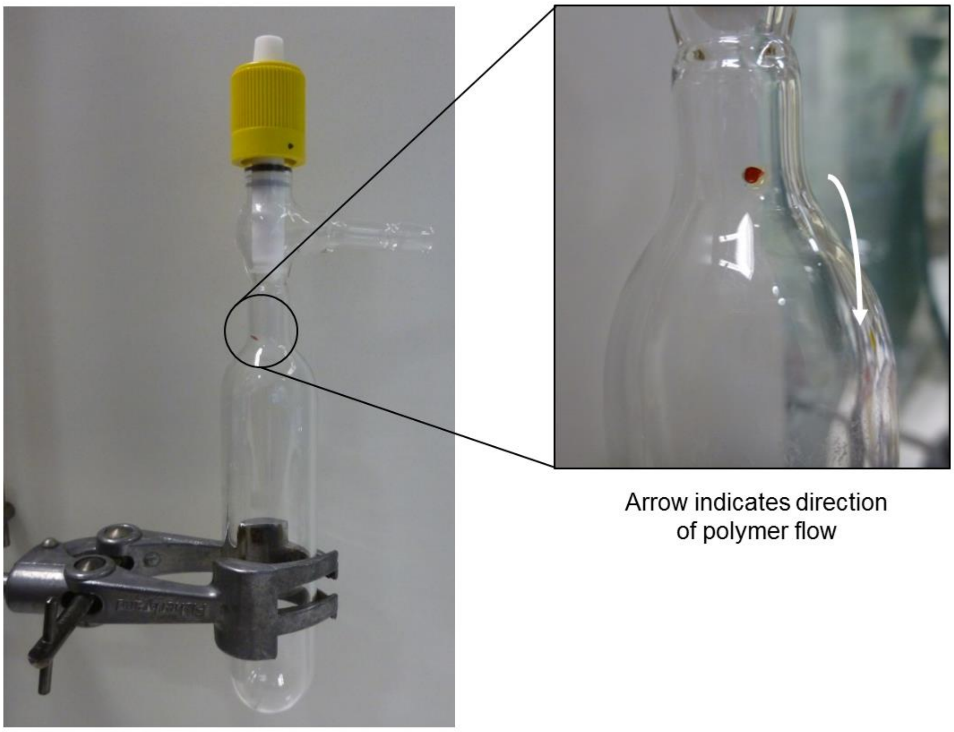

Arrow indicates direction of polymer flow

Figure S24: Image of J. Young NMR set up for Solid-Vapor Polymerization reaction.

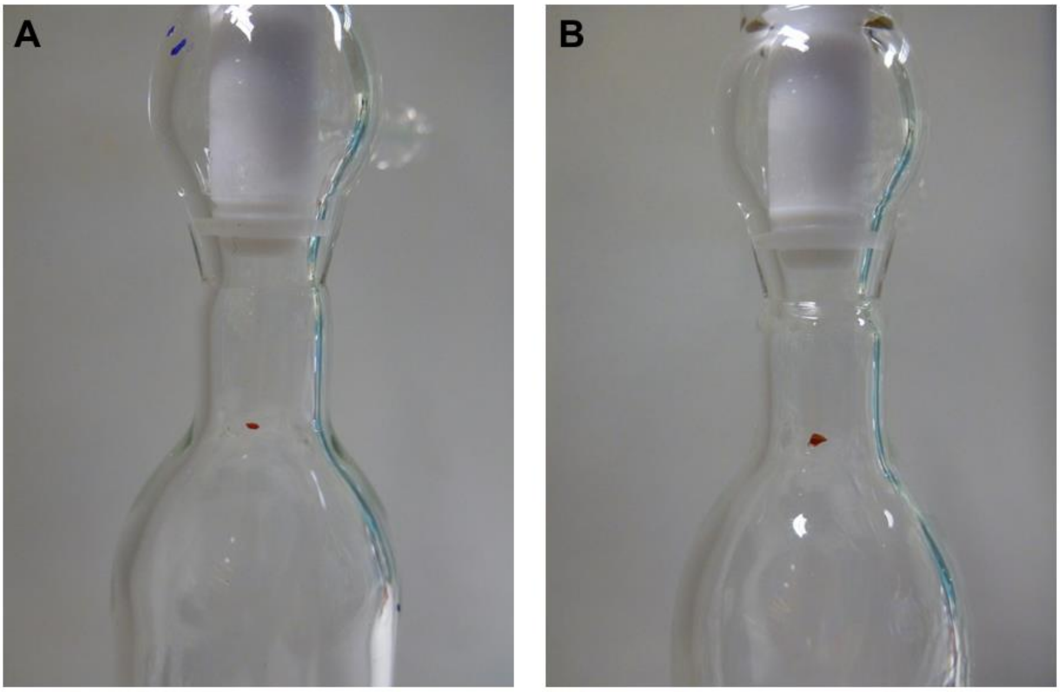

Figure S25: Image of average **(A)** 0.5 mg **(B)** 1.5 mg crystals initiator used in the solid-vapor polymerization reactions.

S.4.2. Solution NMR Spectra

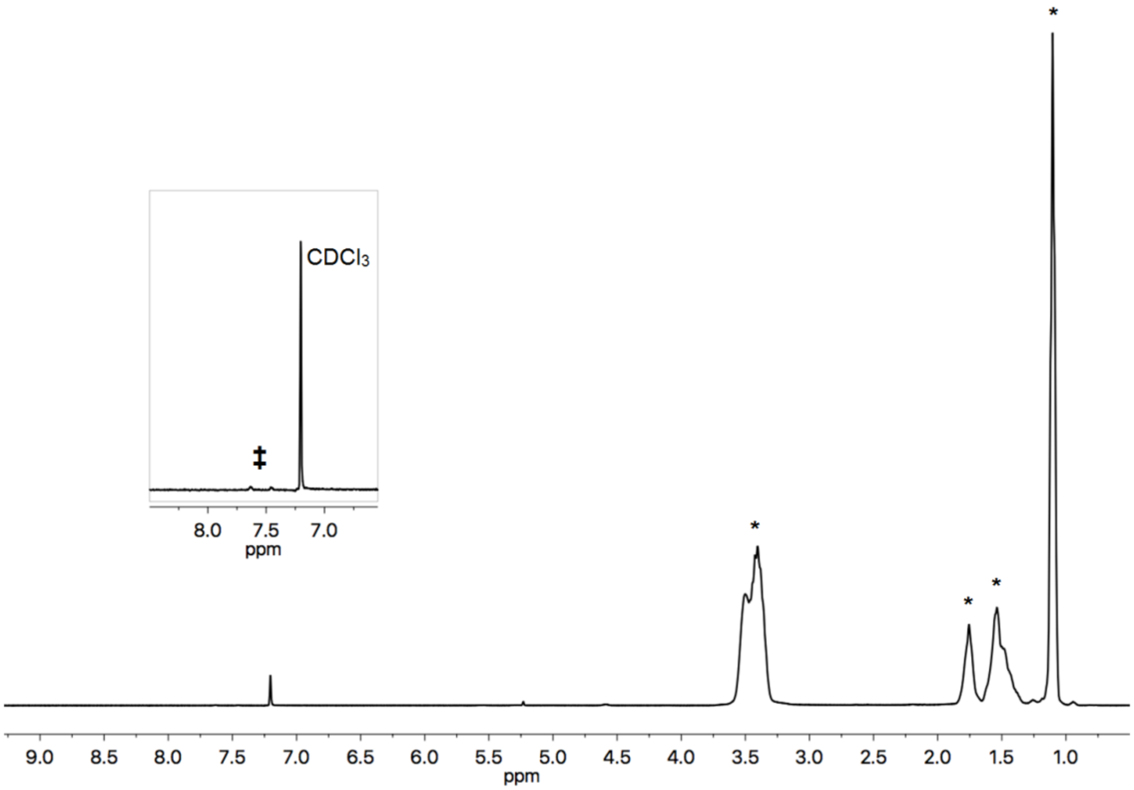

Figure S26: The solution ^{1}H NMR (298 K, $CDCl_3$, 400 MHz) spectrum of **poly(ethylvinylether)** from a solid-vapor polymerization reaction. Peaks marked * are of **poly(ethylvinylether)**.[S6] Insert shows expanded area where small amount of $[BAr^{F}_{4}]^{-}$ anion ^{1}H signals can be seen, marked by ‡.

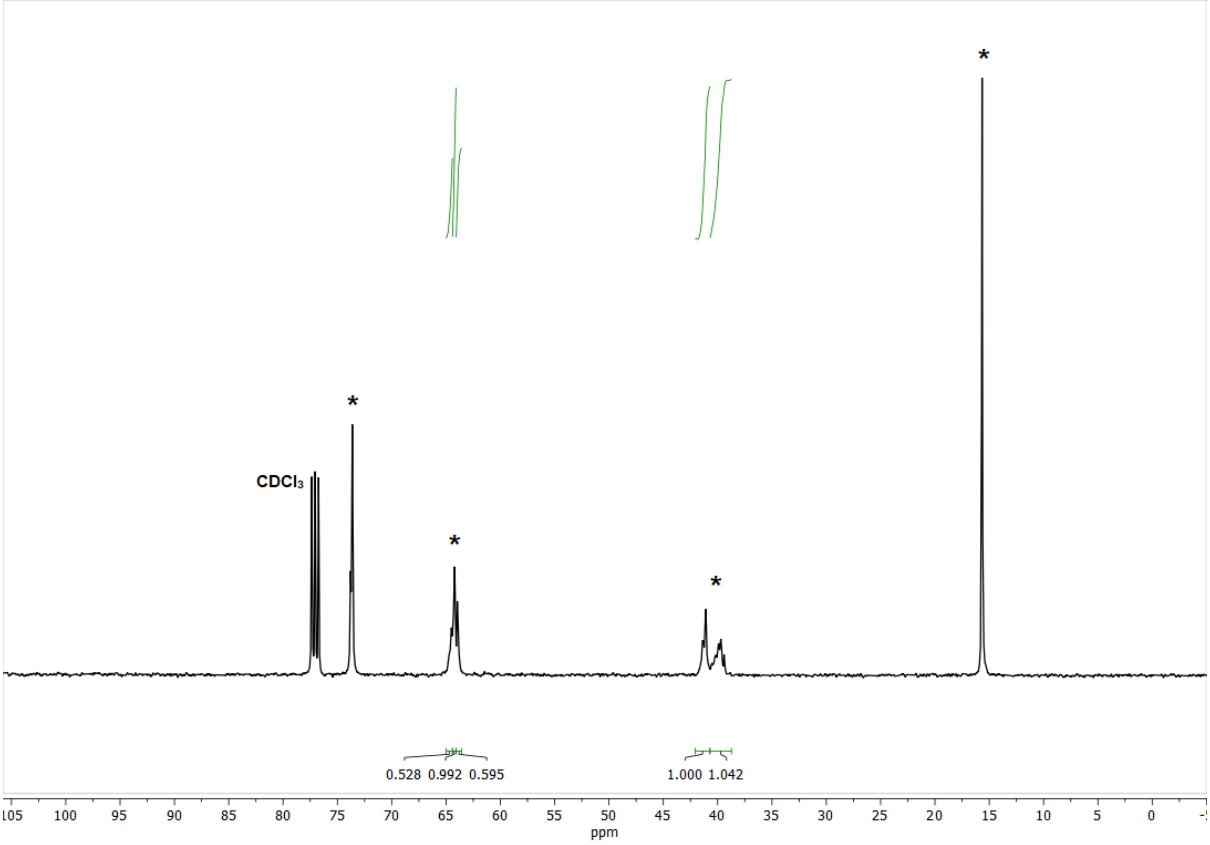

Figure S27: The solution $^{13}C\{^{1}H\}$ NMR spectrum (100 MHz, 298 K,) of **poly(ethylvinylether)** from a solid-vapor polymerization reaction. Peaks marked * are of **poly(ethylvinylether)**.[S6] Integrations of the -**C**H- and -O**C**H_2CH_3 environments highlight atactic nature of **poly(ethylvinylether)**.

S.4.3. GPC Results

Table S1: Table of experiment conditions linking description of initiator conditions to M_n and PDI.

Entry	Initiator Description				Average M_n	Average Đ
	Approx. Crystal Size / mm	Crystal Mass / mgs	Number of Crystals	Approx. Total Crystal Mass / mgs		
1	1.0 × 2.0 × 2.0	1.5	1	1.5	21,500	2.5
2	1.0 × 1.0 × 1.5	1.0	1	1.0	27,200	2.1
3	0.5 × 0.5 × 1.0	0.5	1	0.5	31,800	2.2
4	0.5 × 0.5 × 1.0	0.5	3	1.5	10,900	3.6

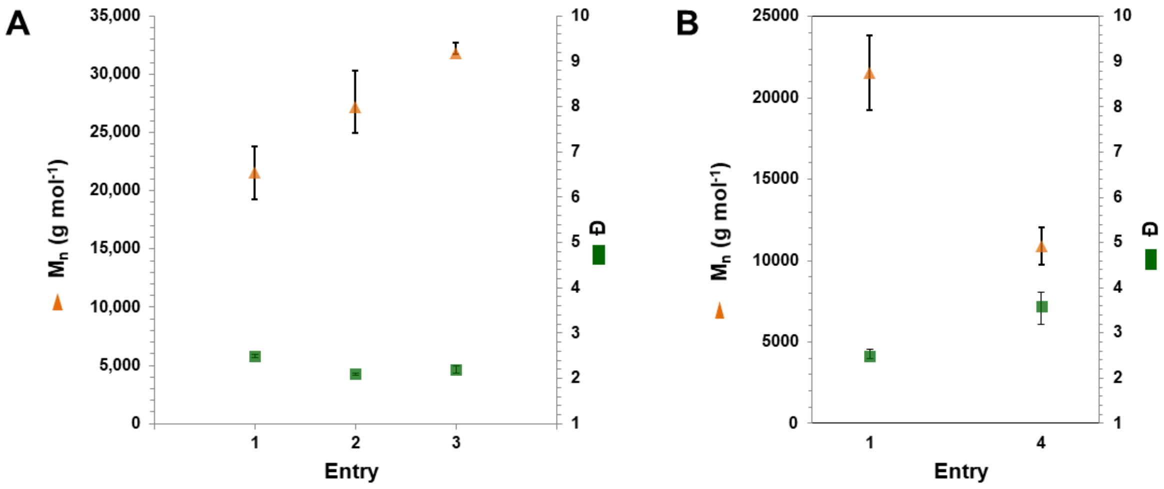

Figure S28: (A) Graph of entries **1** to **3** versus M_n and PDI of the solid-vapour polymerisation reactions. **(B)** Graph plotting reactions **1** and **4** versus M_n and PDI, showing when increasing the surface area by ~ 3 times, yet keeping total initiator mass the same. Entries relate to experimental conditions presented in Table S1.

S.5. New Complexes

S.5.1. $[Rh(Cy_2P(CH_2)_2PCy_2)(Diethyl\ Ether)][BAr^F{}_4]$; $[1\text{-}Et_2O][BAr^F{}_4]$

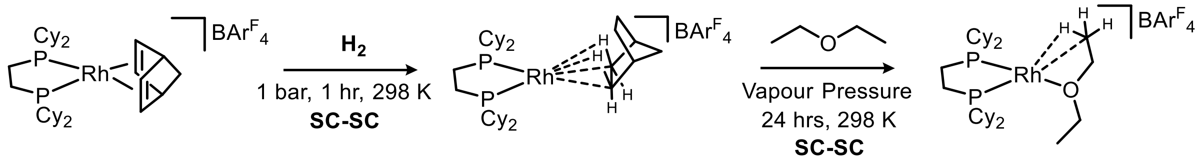

[1-NBD][BAr$^F{}_4$] **[1-NBA][BAr$^F{}_4$]** **[1-Et$_2$O][BAr$^F{}_4$]**

Dark red crystals of **[1-NBD][BAr$^F{}_4$]** (50 mgs) were placed within an glass insert (Figure S29), which in turn was placed inside a J. Young flask (~ 50 mL). This insert was constructed by flame sealing the narrow end of a 150 mm glass Pasteur pipette. The flask was evacuated ($< 3 \times 10^{-2}$ mbar), filled with H_2 gas (15 psi, 298 K) and left to stand for 60 mins, to form **[1-NBA][BAr$^F{}_4$]** *in-situ*.[S2] After this time, the H_2 was removed under vacuum ($< 3 \times 10^{-2}$ mbar) backfilled with argon. Diethyl ether (0.05 mL) was then syringed into the flask, taking care for no liquid diethyl ether to be directly added inside the insert, and therefore come in contact with the crystals directly. The flask was then sealed and a vapor atmosphere of Et_2O was established. After 24 hours, the colour of the crystals had turned a dark brown to yield $[Rh(Cy_2P(CH_2)_2PCy_2)(Et_2O)][BAr^F{}_4]$; **[1-Et$_2$O][BAr$^F{}_4$]**. The crystals were placed under an argon flush for 15 minutes, to remove and excess diethyl ether and transferred to an argon filled glove box and stored at -25 ^oC.

[1-Et$_2$O][BAr$^F{}_4$] was analysed by single crystal x-ray diffraction and $^{31}P\{^1H\}$ / $^{13}C\{^1H\}$ Solid-State NMR spectroscopy. Any attempts to dissolve **[1-Et$_2$O][BAr$^F{}_4$]** in a range of solvents either led to the solvent bound complex (in $F_2C_6H_4$, to give **[1-F$_2$C$_6$H$_4$][BAr$^F{}_4$]**[S1] or in MeCN to give $[Rh(Cy_2PCH_2CH_2PCy_2)(MeCN)_2][BAr^F{}_4]$).[S5] When dissolved in neat Et_2O or CD_2Cl_2, either at 295 or 183 K, formation of the $[BAr^F{}_4]^-$ coordinated zwitterion complex **[1-BAr$^F{}_4$]**[S2] was observed by solution $^{31}P\{^1H\}$ NMR spectroscopy.

$^{31}P\{^1H\}$ SSNMR (162 MHz, 10 kHz spin rate, 298 K): δ 107.0 (d., J_{RhP} 201 Hz, *trans- to the oxygen*)[S7], 99.2 (d., J_{RhP} 223 Hz, *trans- to the agostic interaction)*.[S5]

$^{13}C\{^1H\}$ SSNMR (101 MHz, 10 kHz spin rate, 298 K): δ 163 (ipso-ArC), 134 (br, ortho-ArC), 129 (meta-ArC), 124 (CF_3), 116 (para-ArC), 113.1 (para-ArC), 70 (br, -O**C**H$_2$- of diethyl ether), 42 – 13 (br, multiple aliphatic environments)

Note: Regardless of synthetic method to this compound, a large amount (approximately 50 %) of decomposition to **[1-BAr^F$_4$]**[S2] is observed. This may be due to the high solubility of both **[1-Et$_2$O][BAr^F$_4$]** and **[1-NBA][BAr^F$_4$]** in diethyl ether, which facilitates alkane loss and anion co-ordination in the solid-state during the reaction. Furthermore, Any prolonged period under a dynamic vacuum saw the removal of coordinated Et2O and formation of **[1-BAr^F$_4$]**.[S2]

It was also found bound the norbornadiene in **[1-NBD][BAr^F$_4$]** was not displaced by Et$_2$O. **[1-NBA][BAr^F$_4$]** was essential for this reaction.

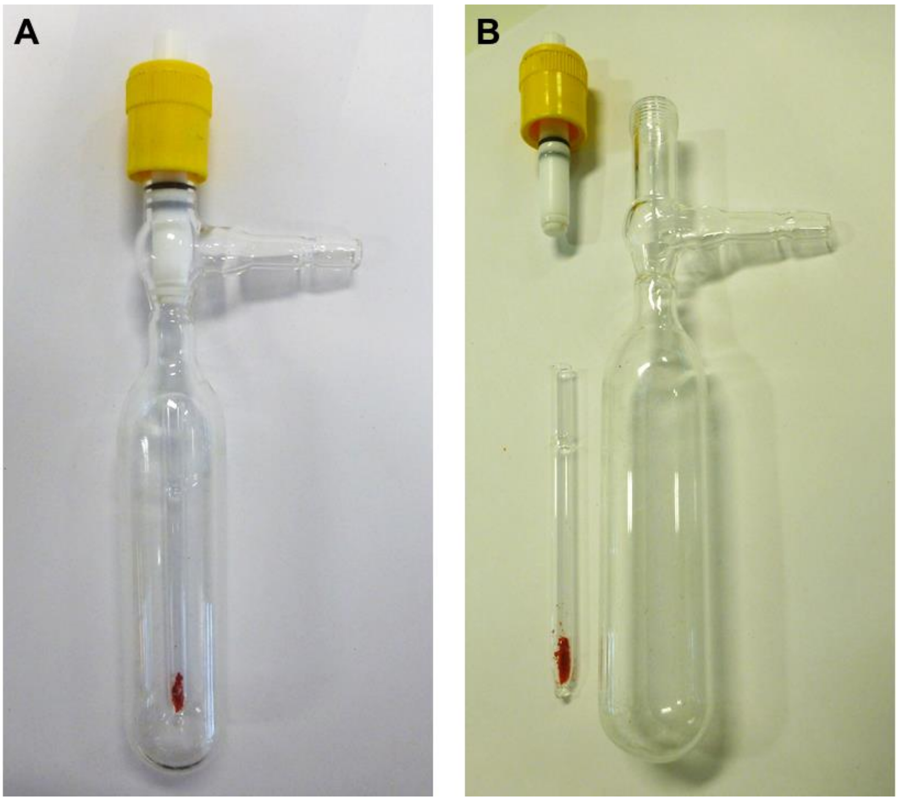

Figure S29: (A) Image of reaction set up of J. Young flask for the synthesis of **[1-Et$_2$O][BAr^F$_4$]**. **(B)** Deconstructed image of **(A)**, showing flame sealed 150 mm glass Pasteur pipette charged with **[1-NBD][BAr^F$_4$]**.

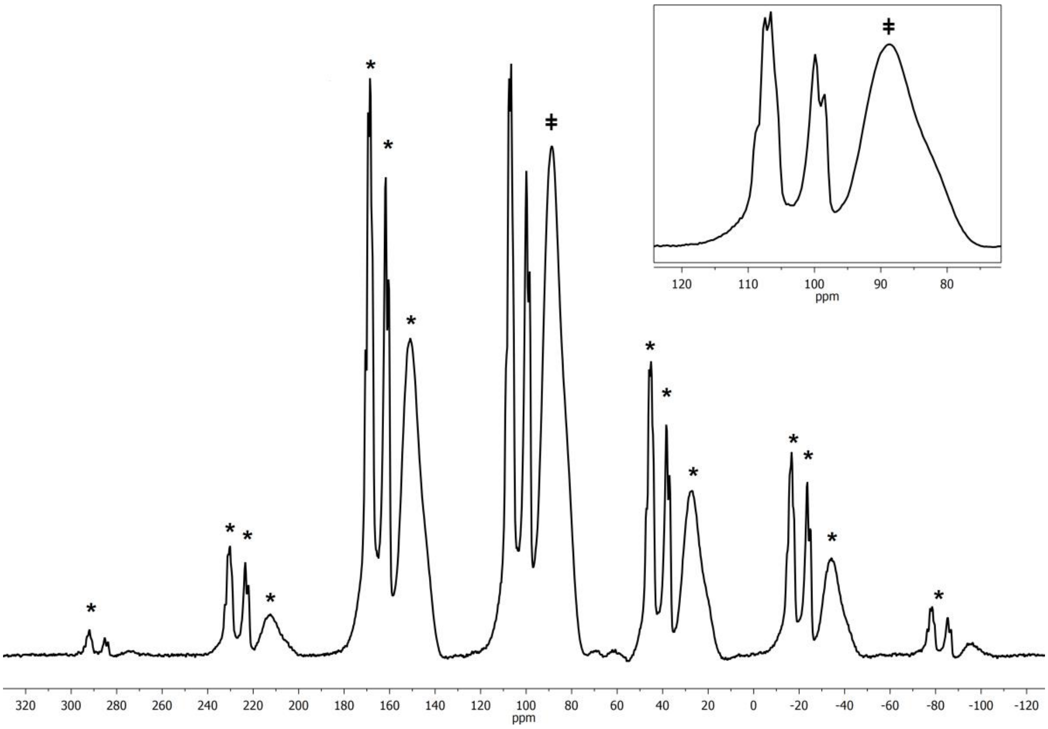

Figure S30: The ^{31}P{^{1}H} SSNMR (162 MHz, 298 K, 10 kHz spin rate) spectrum of **[1-Et$_2$O][BAr$^{F}{}_4$]**. The resonance marked ‡ at 91 ppm is from a considerable amount of decomposition to **[1-BAr$^{F}{}_4$]**.[S2] The inset is a zoom of the resonances at 110 to 90 ppm. The resonances marked ***** are due to spinning sidebands.

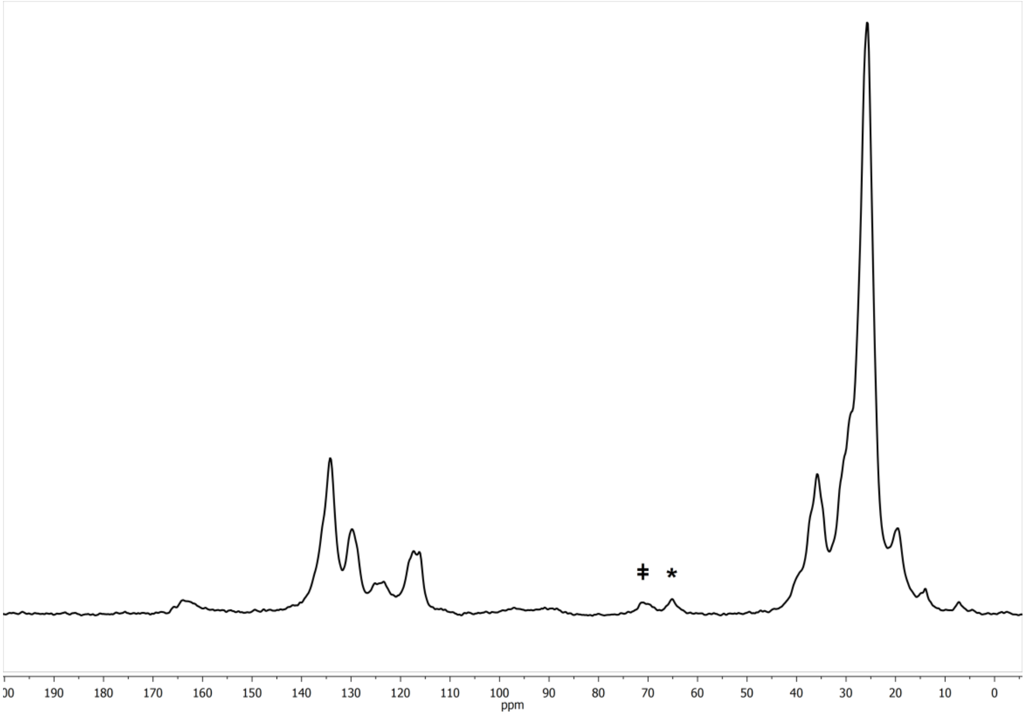

Figure S31: The ^{13}C{^{1}H} SSNMR (100 MHz, 298 K, 10 kHz spin rate) spectrum of **[1-Et$_2$O][BAr$^{F}{}_4$]**. The resonance marked ‡ at 70 ppm is assigned to the -O**C**H$_2$- ^{13}C environment of the bound diethyl ether. The resonances marked ***** are due to spinning sidebands.

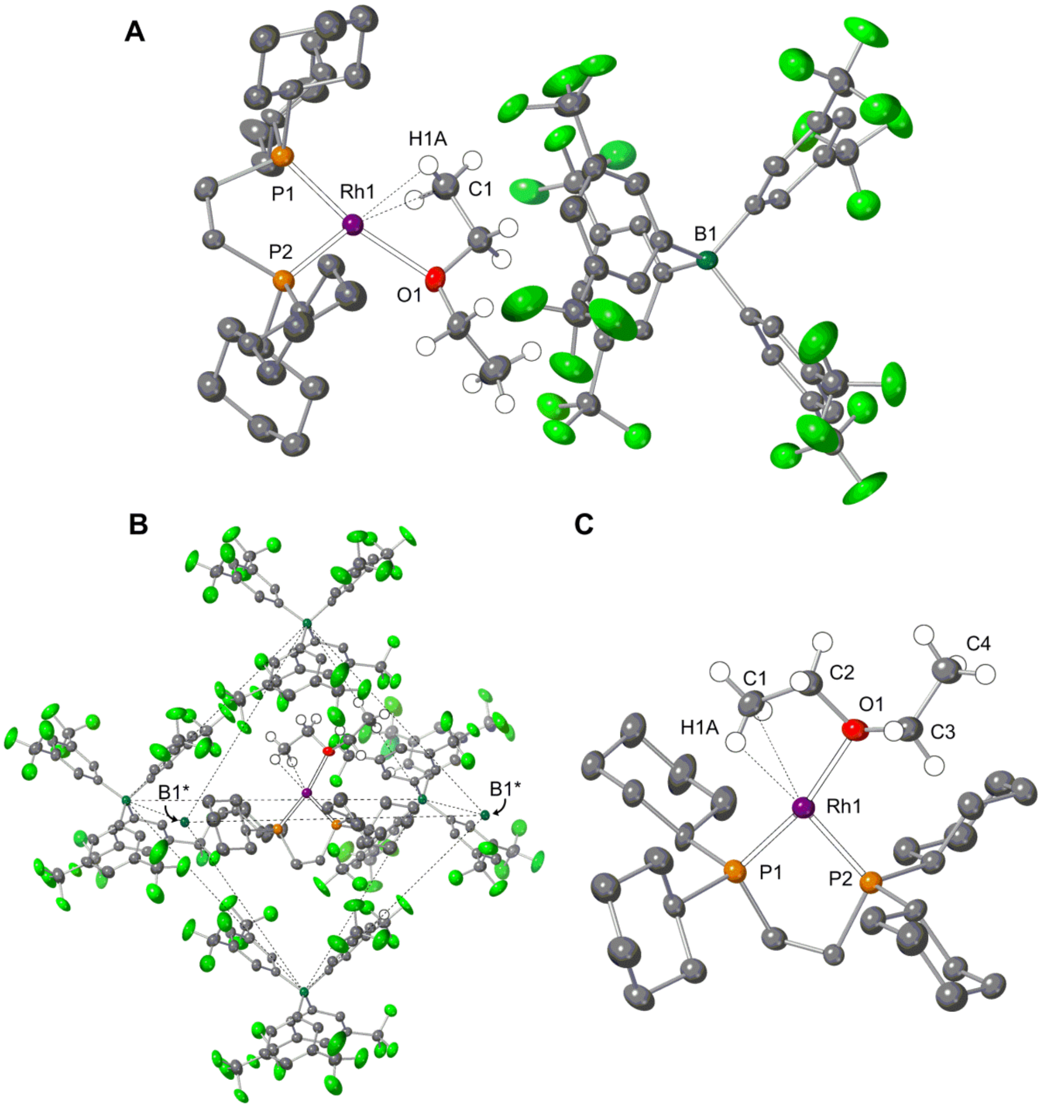

Figure S32: **(A)** Molecular structure of **[1-Et$_2$O][BAr$^F{}_4$]**. **(B)** Structure displaying O$_h$ anion network of the [BAr$^F{}_4$]$^-$ anion, with cationic fragment sat within the cavity; –(Ar$^F{}_4$) removed from 2 boron atoms (marked B1*) for clarity. **(C)** Cationic fragment of **[1-Et$_2$O][BAr$^F{}_4$]**. Displacement ellipsoids set at 30% and hydrogen atoms from phosphine ligand and [BAr$^F{}_4$]$^-$ anion removed for clarity in all parts.

Selected bond lengths (Å): Rh1-P1 2.179(2), Rh1-P2 2.192(2), Rh1-C1 2.522(9), Rh1-H1A 2.180, Rh1-O1 2.204(6).

S.6. Crystallographic and refinement data

S.6.1. Crystal Structure Determinations

Single crystal X-ray diffraction data for all samples were collected as follows: a typical crystal was mounted on a MiTeGen Micromounts using perfluoropolyether oil and cooled rapidly to 150 K in a stream of nitrogen gas using an Oxford Cryosystems Cryostream unit.[S8] Data were collected with an Agilent SuperNova diffractometer (Cu K_α radiation, $\lambda = 1.54180$ Å). Raw frame data were reduced using CrysAlisPro.[S9] The structures were solved using SHELXT[S10] and refined using full-matrix least squares refinement on all F^2 data using the SHELXL-18[S11] using the interface OLEX2.[S12] All hydrogen atoms were placed in calculated positions (riding model). Disorder of CF_3 groups was treated by introducing a split site model and restraining geometries and displacement parameters.

S.6.2. Structures and Refinement Data

Table S2: Selected crystallographic and refinement data.

	[1-NBA][BAr$^F{}_4$] @poly(ethylvinylether)[a]	**[1-NBA][BAr$^F{}_4$] @poly(ethylvinylether)**[b]	**[1-C_3H_6][BAr$^F{}_4$] @poly(ethylvinylether)**	**[1-$C_4H_{10}O$][BAr$^F{}_4$]**
Chemical formula	$C_{65}H_{72}BF_{24}P_2Rh$	$C_{65}H_{72}BF_{24}P_2Rh$	$C_{61}H_{66}BF_{24}P_2Rh$	$C_{62}H_{70}BOF_{24}P_2Rh$
Formula weight	1484.88	1484.88	1430.79	1462.84
Temp. (K)	150.01(10)	150.01(10)	150.1(2)	150.01(10)
Crystal system	Monoclinic	Monoclinic	Triclinic	Triclinic
Space group	$P2_1/n$	$P2_1/n$	P-1	P-1
a (Å)	19.0560(4)	19.0553(10)	12.8015(10)	12.8770(13)
b (Å)	17.9812(5)	18.0135(2)	12.9012(7)	13.5514(7)
c (Å)	19.5544(4)	19.5654(2)	19.8814(9)	19.2488(13)
α (deg)	90	90	91.347(4)	91.699(5)
β (deg)	91.695(2)	91.6800(10)	90.717(5)	95.671(7)
γ (deg)	90	90	96.597(6)	98.347(6)
V (Å^3)	6697.4(3)	6712.99(11)	3260.5(3)	3303.8(4)
Z	4	4	2	2
ρ(calcd) (g cm^{-3})	1.473	1.469	1.457	1.470
μ (mm^{-1})	3.461	3.453	3.532	3.510
Reflections collected	43106	137418	29822	36581
Unique reflections	13896	13967	29822	13564
Restraints / Parameters	264/910	267/894	785 / 971	595 / 989
R_{int}	0.0624	0.0660	0.0535	0.0943
R_1 [$I > 2\sigma(I)$]	0.0752	0.0490	0.1003	0.0900
wR_2 [all data]	0.2155	0.1399	0.3209	0.3020
GooF	1.047	1.044	1.160	1.011
Residual electron density (e Å^{-3})	2.62/-0.89	1.65/-0.56	2.27 / -1.75	1.58 / -1.38
CCDC no.	1022726	1022726	1983128	1983126

[a] Structure collected after 30 seconds exposure to EVE atmosphere. [b] Structure collected after 30 seconds exposure to EVE atmosphere followed by 30 minutes exposure to air. The CCDC numbers for both of these are for the previously published collection of **[1-NBA][BAr$^F{}_4$]**.[S2]

S.7. References

1 F. M. Chadwick, N. H. Rees, A. S. Weller, T. Krämer, M. Iannuzzi and S. A. Macgregor, *Angew. Chemie - Int. Ed.*, 2016, **55**, 3677–3681.

2 S. D. Pike, F. M. Chadwick, N. H. Rees, M. P. Scott, A. S. Weller, T. Krämer and S. A. Macgregor, *J. Am. Chem. Soc.*, 2015, **137**, 820–833.

3 W. L. Earl and D. L. Vanderhart, *J. Magn. Reson.*, 1982, **48**, 35–54.

4 K. Matsuzaki, H. Ito, T. Kawamura and T. Uryu, *J Polym Sci Part A-1 Polym Chem*, 1973, **11**, 971–987.

5 F. M. Chadwick, A. I. McKay, A. J. Martinez-Martinez, N. H. Rees, T. Krämer, S. A. Macgregor and A. S. Weller, *Chem. Sci.*, 2017, **8**, 6014–6029.

6 L. Lin, G. Zhang, K. Kodama, H. Shitara and T. Hirose, *J. Polym. Sci. Part A Polym. Chem.*, 2016, **54**, 861–870.

7 A. Kumar, N. A. Beattie, S. D. Pike, S. A. Macgregor and A. S. Weller, *Angew. Chemie - Int. Ed.*, 2016, **55**, 6651–6656.

8 B. J. Cosier and A. M. Glazer, *J. Appl. Crystallogr.*, 1986, **19**, 105–107.

9 *Oxford Diffraction Ltd.*, 2011.

10 G. M. Sheldrick, *Acta Crystallogr. Sect. A Found. Crystallogr.*, 2008, **64**, 112–122.

11 G. M. Sheldrick, *Acta Crystallogr. Sect. A Found. Crystallogr.*, 2015, **71**, 3–8.

12 O. V. Dolomanov, L. J. Bourhis, R. J. Gildea, J. A. K. Howard and H. Puschmann, *J. Appl. Crystallogr.*, 2009, **42**, 339–341.